

# Light Water Reactor Sustainability Program

## Cable Nondestructive Examination Online Monitoring for Nuclear Power Plants



September 2020

U.S. Department of Energy  
Office of Nuclear Energy

#### **DISCLAIMER**

This information was prepared as an account of work sponsored by an agency of the U.S. Government. Neither the U.S. Government nor any agency thereof, nor any of their employees, makes any warranty, expressed or implied, or assumes any legal liability or responsibility for the accuracy, completeness, or usefulness, of any information, apparatus, product, or process disclosed, or represents that its use would not infringe privately owned rights. References herein to any specific commercial product, process, or service by trade name, trade mark, manufacturer, or otherwise, does not necessarily constitute or imply its endorsement, recommendation, or favoring by the U.S. Government or any agency thereof. The views and opinions of authors expressed herein do not necessarily state or reflect those of the U.S. Government or any agency thereof.

# **Cable Nondestructive Examination Online Monitoring for Nuclear Power Plants**

**Authors: S.W. Glass<sup>1</sup>, L.S. Fifield<sup>1</sup>, Nicola Bowler<sup>2</sup>**

**<sup>1</sup> Pacific Northwest National Laboratory**

**<sup>2</sup> Iowa State University**

**September 2020**

**Prepared for the  
U.S. Department of Energy  
Office of Nuclear Energy**

## Summary

This Pacific Northwest National Laboratory (PNNL) milestone report describes investigation into cable inspection and monitoring methods that may be adapted to nuclear power plant online monitoring. There are numerous nondestructive examination (NDE) methods to assess the condition of power plant cables. Most of these methods, however, require the cable systems to be offline and, in many cases, separated from their load. The challenge for online systems is to test the cable system without applying voltage and current that can damage or interrupt normal system function. There are numerous advantages to online monitoring if conditions of interest can be effectively detected early enough to manage or mitigate failure risk. These include:

- Continuous or frequent interrogation of the cable circuit may detect system degradation much earlier than a periodic manual check applied during outage or offline test periods that may be one to several years apart.
- Online monitoring supports trending and differential measurements that can look for subtle changes between the initial state when monitoring is first started and the current or latest measurement.
- Online monitoring can be the only way to detect and locate certain intermittent faults such as those associated with operational vibration or conditions like elevated temperature, operational stress and strain, or electrical load.
- Manual testing normally requires human intervention to separate the cable systems from motor and sensor loads, which must be scheduled to minimize system availability interruption. There is also a significant risk of human error either in workmanship associated with re-terminating cable ends, improper test implementation, or in re-connecting circuits incorrectly.
- The initial cost of an online monitoring system (hardware, installation, and adjusting plant operating procedures to include checking the system) may exceed the cost of one to several manual inspections. However, long-term costs may be lower from reduction in manual inspection interventions.

Candidate technologies for online monitoring of nuclear power plant (NPP) cables fall into the following major categories:

- Electrical reflectometry (time-domain reflectometry [TDR], spread-spectrum time-domain reflectometry, frequency-domain reflectometry, joint-time/frequency-domain reflectometry)
- Cable-as-waveguide partial discharge measurements
- Fiber optics (temperature profile, mechanical strain associated with mechanical loads, acoustic strain associated with partial discharge)
- External jacket/insulation measurement (interdigital capacitance, indenter modulus, ultrasound, Fourier transform infrared spectroscopy [FTIR], Fourier transform near-infrared spectroscopy [FT-Near IR])

To date, there are few examples of online test and monitoring applications applied to low- and medium-voltage (MV) nuclear power plant circuits. This report addresses the technology classes above, as well as several examples related to nuclear and relevant industrial applications. In particular:

- Online noise monitoring and TDR used to diagnose a source range detector circuit.
- Online noise monitoring and TDR used for rod drop clamp ratchet detection

- High-voltage (HV) and MV use of the cable as a waveguide for partial discharge detection and location
- HV fiber optic monitoring of partial discharge
- HV fiber optic monitoring of temperature profile

The feasibility for online monitoring to detect several cable fault types of interest has been established by various labs, universities, and commercial entities using a variety of methods. Among the techniques examined above, some are already being applied to HV and critical-cable systems. Broad application of these techniques, however, has not extended to MV and low-voltage (LV) cable systems of industrial or nuclear plants as a common practice. Exploitation of these technologies for a broader range of cables will require additional research to reduce equipment, installation, and operating costs.

## **Acknowledgments**

Funding for this work is provided by the U.S. Department of Energy, Office of Nuclear Energy, Light Water Reactor Sustainability Program, Materials Research Pathway under the leadership of T.M. Rosseel.

Pacific Northwest National Laboratory (PNNL) is a multi-program national laboratory operated for the U.S. Department of Energy by Battelle Memorial Institute.

The work performed by Iowa State University was performed under a subcontract from PNNL.

# Contents

Summary .....	i
Acknowledgments.....	iii
Contents .....	iv
Figures .....	v
Tables.....	vi
Acronyms and Abbreviations .....	vii
1. Objectives .....	1
2. Technologies for Online Cable Condition Monitoring.....	3
2.1 Time, Frequency, Sequence, and Spread Spectrum Reflectometry .....	3
2.1.1 Time Domain Reflectometry .....	3
2.1.2 Sequence/Spread Spectrum Time Domain Reflectometry.....	4
2.1.3 Frequency Domain Reflectometry .....	8
2.1.4 Comparison of reflectometry methods.....	9
2.2 Partial Discharge Detection with Cable as Waveguide.....	11
2.3 Fiber Optic Temperature and Acoustic Measurements.....	16
2.3.1 Bragg Grating Measurements .....	16
2.3.2 Distributed Optical Fiber Sensors .....	16
2.3.3 Rayleigh Scattering.....	17
2.3.4 Brillouin Scattering.....	18
2.3.5 Raman Scattering .....	19
2.3.6 Commercial Fiber Optic Instrumentation .....	19
2.4 IDC Sensors for Online Monitoring.....	22
3. Examples of Online monitoring Fault Detection.....	28
3.1 TDR Rod Control System Coil and Cable Testing in an NPP .....	28
3.2 TDR Intermittent Fault Identification in a Nuclear Power Plant Instrument Cable.....	28
3.3 MV Partial Discharge Monitoring/Trending with Cable as Waveguide .....	29
3.4 HV Fiber Optic Monitoring of Temperature Profile.....	30
3.5 Fiber Optic Monitoring of PD.....	31
4. Conclusions .....	33
5. References .....	34

## Figures

Figure 2-1. Typical TDR 3-Conductor Test Plot. RTD: resistance temperature sensor. (IAEA 2012).....	4
Figure 2-2. S/SSTDR circuit diagram.....	5
Figure 2-3. STDR and modulated SSTDR signals. ....	5
Figure 2-4. Autocorrelations of STDR and SSTDR signals from Figure 2-3.....	6
Figure 2-5. Correlator output for STDR and SSTDR tests on $75\Omega$ coax cable with an open circuit 23 m down the cable. Note the peak at zero (connection between the test system and cable), multiple reflections, and definitive shape of the correlation peaks.....	6
Figure 2-6. (a) STDR and (b) SSTDR correlation response for an open circuit measured on two 22 AWG loosely bundled wires that are 9.9 m long.....	7
Figure 2-7. STDR response for an 80 ft wire with end open and short .....	7
Figure 2-8. General FDR test uses 2 conductors to interrogate conductor and insulation-based cable impedance changes (Glass et al. 2016) .....	8
Figure 2-9. Typical offline tan delta and partial discharge connection configuration. VLF – very low frequency .....	12
Figure 2-10. Typical online partial discharge monitoring configuration.....	12
Figure 2-11. PD equivalent circuit with a void containing PD .....	13
Figure 2-12 Graphical representation of voltage appearing across device under test showing PD beginning when $U_A$ exceeds inception voltage and ending when it drops below extinction voltage.....	13
Figure 2-13. Change in Bragg grating distance can be proportional to change in temperature or strain .....	16
Figure 2-14. Distributed temperature and strain fiber optic sensing based on changes in reflections from anomalies along the full length of the fiber as indicated by Raman and Brillouin peaks. Location information is based on reflection time delay .....	17
Figure 2-15. A notional COTDR system showing the source, modulator, local oscillator, backscattered signal, and detector .....	18
Figure 2-16. Fiber shaping signal amplitude as a function of angle of incidence $\theta$ for a cable with a straight fiber (green), a helical fiber (red) and a linear combination of helical plus straight for two ground conditions (Lumens et al. 2013). For soil harder than that encountered, the response would follow the dotted lines. All curves normalized based on the response at $\theta = 0^\circ$ of a cable with a straight fiber (Lumens 2014) (Lumens et al 2013).....	21
Figure 2-17. Shot record of three located sensor systems: (a) vertical accelerometer, (b) a straight fiber, (c) a shaped fiber. White arrows point to reflected energy, not present on the straight fiber plot, and the red arrows in the shaped fiber plot point to ground roll from ambient noise sources (Lumens 2014).....	21
Figure 2-18. Plastic spring-loaded clamp sensor with inset showing detail of the jaws and interdigital electrodes attached to both orange jaws (Sheldon and Bowler, 2014).....	22
Figure 2-19. Illustration of possible NPP configuration with numerous surface mount IDC sensors deployed for continuous monitoring of cable health .....	23

Figure 2-20. Illustration of patch IDC sensor with auxiliary components necessary for a continuous cable health monitoring system.....	23
Figure 2-21. Schematic presentation of frequency dependence of permittivity for typical relaxation modes in polymers (Bowler and Liu, 2015) .....	24
Figure 2-22. (a) Unjacketed cable cross section with IDC, (b) jacketed cross section, (c) orthogonal view of IDC (Glass III et al. 2018).....	26
Figure 2-23. Finite element simulation of field penetration depth as a function of tine gap (Glass III et al. 2018) .....	26
Figure 2-24. Pink EPR insulation; CPE jacket aged samples with jacket removed from half of the sample (Glass III et al. 2018).....	26
Figure 2-25. Linear least squares correlation of measured (on-insulation) vs. predicted (through jacket) dissipation factor which is shown to indicate insulation condition.....	27
Figure 3-1. TDR traces locating a movable gripper coil short circuit on reactor head.....	28
Figure 3-2. Intermittent fault location in an energized source range neutron detector circuit at 1,500 VDC normal operating voltage in laboratory test environment.....	29
Figure 3-3. 3-D graph of developing PDs in a flawed joint with a crimped connector running hot at 1,678 m along the circuit length (Cuppen, Steennis, and van der Wielen 2010).....	30
Figure 3-4. Fiber optic receiver signal and conventional partial discharge sensor responses to a 40 kV applied test voltage (Tian et al. 2005).....	31
Figure 3-5. Optical sensor PD signal from real production defect (void) between stress shield and epoxy resin within the 400 kV cable joint (Tian et al. 2005) .....	32
Figure 3-6. Optical sensor PD signal due to PD from wires within the cable joint of 400 kV cable at 70 kV (Tian et al. 2005).....	32

## Tables

Table 2-1. Cable/cable health related and cable test/environmental related FDR influence parameters.....	8
Table 2-2. Comparison of reflectometry methods .....	9
Table 2-3. Companies and products for electrical, thermal, IR, UV, and acoustic PD monitoring.....	15
Table 2-4. Selection (not comprehensive) of companies offering commercial off-the-shelf fiber optic instrumentation systems.....	20

## Acronyms and Abbreviations

AC	alternating current – normally 50 or 60 Hz
AE	airborne acoustic emission
FMCW	frequency modulated continuous wave
COTDR	coherent optical time domain reflectometry
CPE	chlorinated polyethylene
D	electric displacement
DITEST	distributed temperature test
DS	dielectric spectroscopy
DTS	distributed temperature sensor
DUT	device under test
$\epsilon$	complex permittivity composed of $\epsilon'$ (real part) and $\epsilon''$ (imaginary part)
$\mu\epsilon$	micro-strain (change in length/nominal length) x 10 <sup>-6</sup>
EAB	elongation-at-break
EPR	ethylene-propylene rubber
f	frequency
F	international system of units of electrical capacitance (farad) named after English physicist Michael Faraday (1791-1867)
FFT	fast Fourier transform
FTIR	Fourier transform infrared spectroscopy
FT-Near IR	Fourier transform near-infrared spectroscopy
Gy	gray (unit measure of ionizing radiation)
HV	high voltage (> 35 kV)
Hz	hertz (1 Hz = 1 cycle/sec)
IAEA	International Atomic Energy Association
I&C	instrumentation and control
IDC	interdigital capacitor or interdigital capacitive
IR	infrared (as IR thermal imaging)
IM	indenter modulus
kV	kilovolts
ML Code	maximum length (for S/SSTDR, this is typically 1,023-bit PN code)
MSR	magnitude detection-mixed signal reflectometry
MV	medium voltage (1,000 V to 35 kV)
NDE	nondestructive evaluation
NIS	nuclear instrumentation system

NPP	nuclear power plant
O&M	operations and maintenance
PD	partial discharge
PN Gen	pseudo-noise digital sequence generator
PNNL	Pacific Northwest National Laboratory
PVC	polyvinyl chloride
RTD	resistance temperature sensor
SHM	state-of-health monitoring
SSTDR	spread spectrum time domain reflectometry
STDTR	sequenced time domain reflectometry
SWR	standing wave reflectometry
Tan Delta	dielectric loss tangent; also known as dissipation factor
TDR	time domain reflectometry
UV	ultraviolet
V	volts
VLF	very low frequency
XLPE	cross-linked polyethylene
$\chi$	electrical susceptibility

# 1. Objectives

This Pacific Northwest National Laboratory (PNNL) milestone report describes research into cable inspection and monitoring methods that may be adapted to nuclear power plant online monitoring.

Maintaining an NPP requires very labor-intensive activities to meet high safety standards. Under current energy-market conditions, the nuclear industry must innovate and move towards a more economically viable approach. This will require reducing operations and maintenance (O&M) cost by minimizing labor involved and frequency of O&M activities. This could include automating activities such as maintenance work processes, operations surveillances, or support activities like administration, security, and radiation protection (Rashdan et al. 2018).

There are numerous nondestructive examination (NDE) methods to assess the condition of power plant cables. Most of these methods require the cable systems to be offline and, in many cases, separated from their load (Glass et al. 2015). The challenges for online systems are testing cables without applying voltage or current that can damage or interrupt normal system function and protecting test instruments from line or signal voltage and frequency (typically 120 V–35 kV/50–60 Hz). There are numerous advantages to online monitoring that can effectively detect conditions of interest early enough to manage or mitigate failure risk. These include:

- Continuous or frequent interrogation of the cable circuit may detect system degradation much earlier than a periodic manual check applied during outage or offline test periods that may be one to several years apart.
- Online monitoring supports trending and differential measurements that can look for subtle changes between the initial state when monitoring is initiated and the current or latest measurement.
- Online monitoring can be the only way to detect and locate certain intermittent faults such as those associated with operational vibration or conditions like elevated temperature, operational stress and strain, or electrical load.
- Manual testing normally requires human intervention to separate the cable systems from motor and sensor loads, which must be scheduled to minimize system availability interruption. There is also a significant risk of human error due to workmanship associated with re-terminating cable ends, improper test implementation, or in re-connecting circuits incorrectly.
- The initial cost of an online monitoring system (hardware, installation, and adjusting plant operating procedures to include checking the system) may exceed the cost of one to several manual inspections. However, long-term costs may be lower from reduction in manual inspection interventions.

Candidate technology for online monitoring of NPP cables falls into the following major categories:

- Electrical reflectometry (time-domain reflectometry [TDR], spread-spectrum time-domain reflectometry, frequency-domain reflectometry, joint-time/frequency-domain reflectometry)
- Cable-as-waveguide partial discharge measurements
- Fiber optics (temperature profile, mechanical strain associated with mechanical loads, acoustic strain associated with partial discharge)
- External jacket/insulation measurement (interdigital capacitance, indenter modulus, ultrasound, Fourier transform infrared spectroscopy [FTIR], Fourier transform near-infrared spectroscopy [FT-Near IR])

To date, there are few examples of online test and monitoring applications applied to low- and medium-voltage (MV) nuclear power plant circuits. This report addresses the technology classes listed above, as well as several examples that have been found related to nuclear and industrial applications. In particular:

- Online noise monitoring and TDR used to diagnose source range detection
- Online noise monitoring and TDR used for rod drop clamp ratchet detection
- High-voltage (HV) and MV use of the cable as a waveguide for partial discharge detection and location
- HV fiber optic monitoring of partial discharge
- HV fiber optic monitoring of temperature profile

The overall objective of this project are to develop the technical basis for assessing the level and impact of cable insulation aging and degradation in NPPs. In July of 2012, a workshop (Simmons et al. 2012) was held to lay the groundwork for a research and development roadmap to address aging cable management in NPPs, including methods for nondestructively measuring the condition of aging cables. The project addresses the overall gaps that were identified at that workshop using a phased approach. This phased approach addresses the three areas identified from the workshop:

1. Determine key indicators of cable aging. This has largely been addressed in earlier reports (Ramuhalli et al. 2015, Simmons et al. 2014, Fifield et al. 2015).
2. Characterize and advance current NDE methods and develop new NDE methods using insights from the determination of key indicators. This activity was generally addressed by Glass et al. (2015) describing the overall state of the art for both bulk electrical tests and local tests. More focused reports have been prepared to address local NDE cable tests (Glass, Fifield, and Hartman 2016); bulk and distributed cable tests, particularly focusing on frequency domain reflectometry (Glass et al. 2017), and interdigital capacitance (IDC) (Glass III et al. 2018). A separate report (Glass, Fifield, et al. 2019) continued efforts to characterize and advance NDE methods, focusing on cable capacitance and dielectric spectroscopy (DS). This report addresses online methods.
3. Develop models that use advances in key indicators and NDE methods to help predict the remaining life of cables. Modeling has been and continues to be essential to understand the relevance and aid in the interpretation of NDE results. Examples of this include Glass, Fifield, and Hartman (2016), Glass III et al. (2018), as well as the DS report (Glass, Fifield, et al. 2019).

This report is submitted in fulfillment of deliverable M3LW-20OR0404023 report on Cable Nondestructive Examination Online Monitoring for Nuclear Power Plants.

## **2. Technologies for Online Cable Condition Monitoring**

### **2.1 Time, Frequency, Sequence, and Spread Spectrum Reflectometry**

#### **2.1.1 Time Domain Reflectometry**

Time domain reflectometry (TDR) measures reflections of a stepped or impulse signal along a single conductor to detect and locate any changes in the conductor impedance (Glass et al. 2015). A TDR pulse is usually less than 10 volts and is primarily in the higher frequency range of > 1 kHz, so the pulse has little or no effect on low frequency signals or on 60 Hz power excitation. TDR transmits an incident signal into the conductor and listens for signal reflections. If the conductor is a uniform impedance network and is properly terminated to matching impedance, then there will be no reflections and the transmitted signal will be completely absorbed at the far end by the termination. Instead, if there are impedance variations as in a short or open circuit at the cable end, a damaged or reduced cross-sectional area, or a splice with a higher resistance along the conductor, then some fraction of the incident signal will be reflected back to the source. The polarity of the reflection contains information about the reflector. An open cable end will reflect “in-phase” with the excitation and a short will reflect as an inverted signal. This reflected signal is measured at a point in time on the TDR instrument that is proportional to the signal propagation velocity in the cable and the distance along the cable, thereby allowing assessment of the location of any reflector observed. The amplitude of the reflected signal coupled with the inherent cable attenuation characteristics also allows an estimate of the magnitude of the impedance change. An example TDR test setup and plot is shown in Figure 2-1 (IAEA 2012).

TDR testers are portable units that can easily be used in-situ within an NPP. The test is a low-voltage (LV) test so there is virtually no risk to the cable. The main emphasis, however, of a portable TDR tester is to assess cable condition, faults, or anomalies in the conductor. Very little information is provided regarding subtle changes in the insulation as would be anticipated from early stages of cable aging insulation degradation. Moreover, these units are not intended to be operated on live wires and in fact most have a warning indication if a voltage is detected on the test wire (Megger 2020).

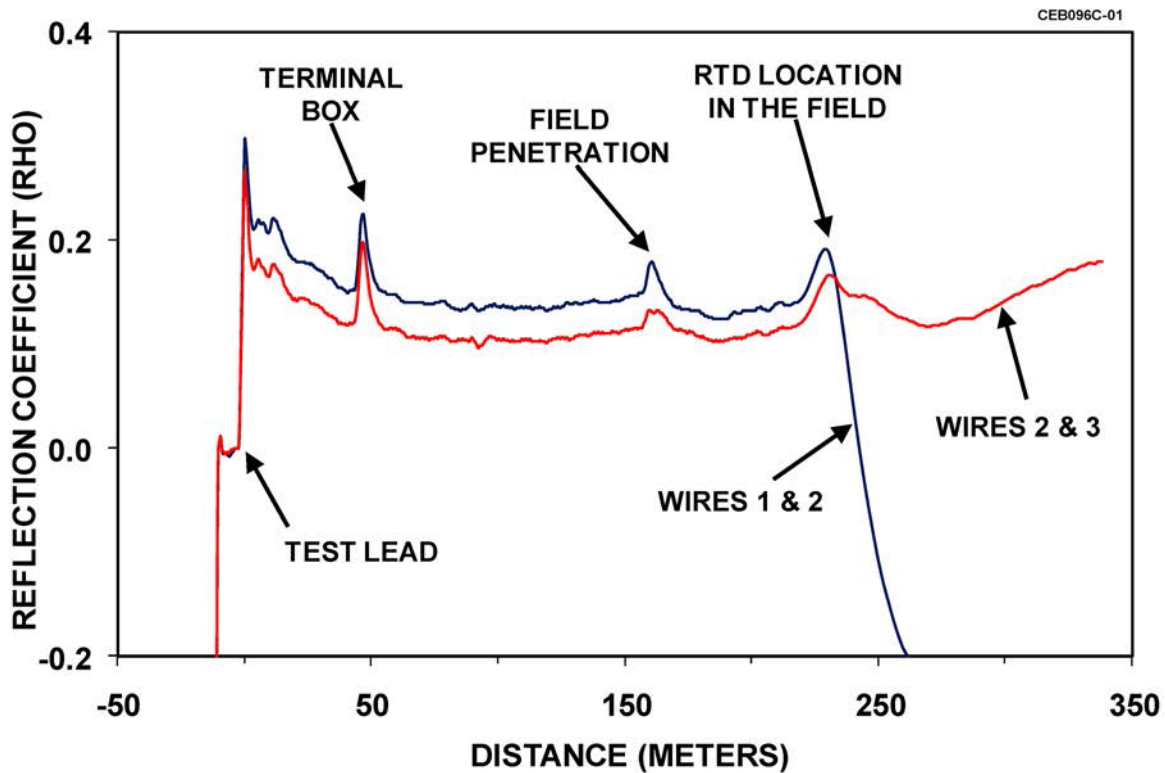
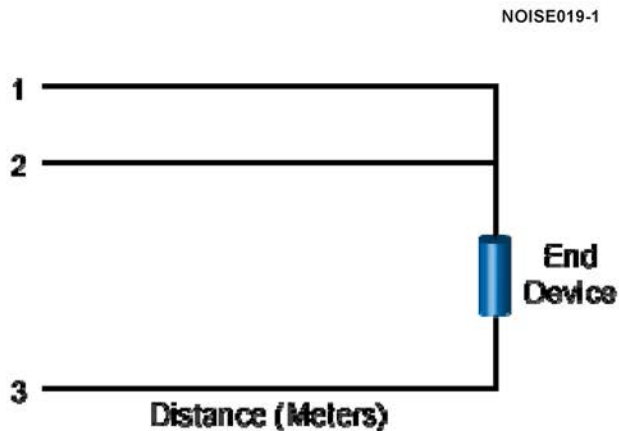


Figure 2-1. Typical TDR 3-Conductor Test Plot. RTD: resistance temperature sensor. (IAEA 2012)

### 2.1.2 Sequence/Spread Spectrum Time Domain Reflectometry

Several methods are available today for locating electrical faults fundamentally based on reflectometry concepts. These include TDR as discussed above, frequency domain reflectometry (FDR) (Glass et al. 2017) (Smith, Furse, and Kuhn 2008) (Furse et al. 2003), standing wave reflectometry (SWR), mixed signal reflectometry (MSR) (Tsai et al. 2005), multicarrier reflectometry (MCR) (Naik, Furse, and Boroujeny 2006) and sequence/spread spectrum time domain reflectometry (S/SSTDR) (Smith, Furse, and Kuhn 2008). For online applications, S/SSTDR has been most fully exploited in the aircraft industry. A block diagram of S/SSTDR is shown in Figure 2-2. A sine wave generator (operating at 30–100 MHz) creates the master system clock. Its output is converted to a square wave via a waveform shaper and the resulting square wave drives a pseudo-noise digital sequence generator (PN Gen) Figure 2-3.

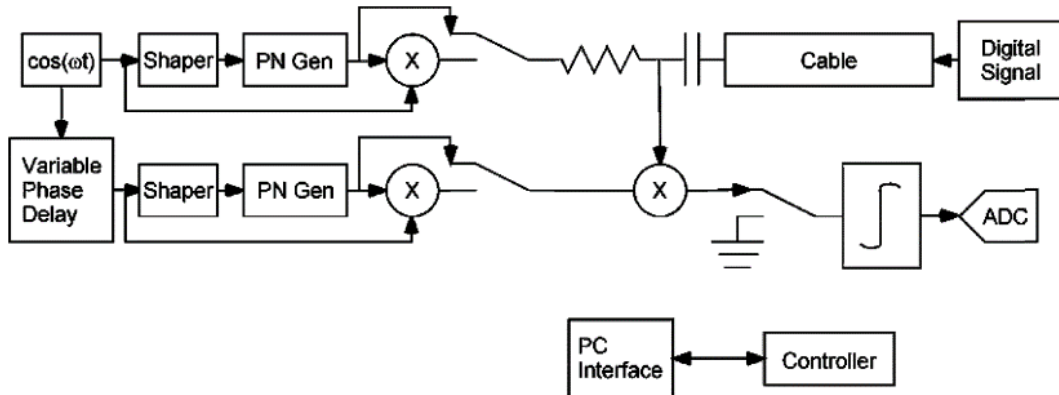


Figure 2-2. S/SSTDR circuit diagram.

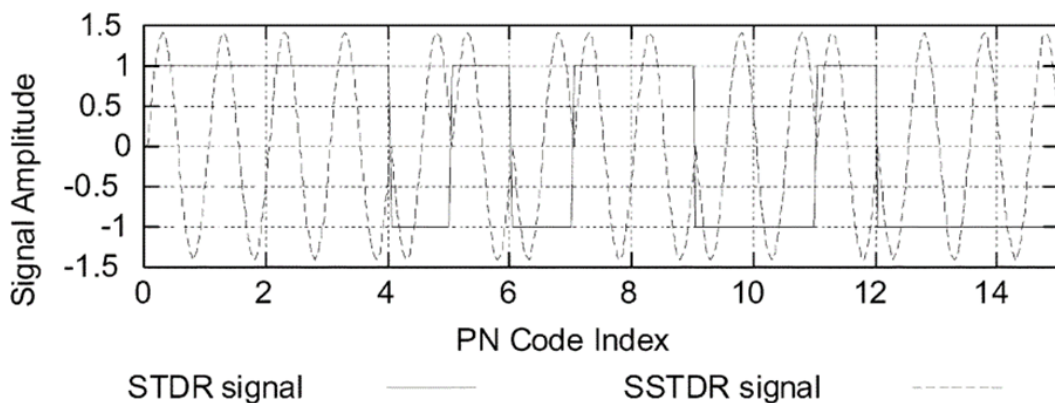


Figure 2-3. STDR and modulated SSTDR signals.

To use spread SSTDR, the sine wave is multiplied by the output of the PN generator, generating a direct sequence spread spectrum binary phase shift keyed signal. To use STDR, the output of the PN generator is not mixed with the sine wave; the test signal is injected into the cable. The total signal from the cable (including any digital data or alternating current [AC] signals on the cable, and any reflections observable at the receiver) is fed into a correlator circuit along with a reference signal. The received signal and the reference signal are multiplied, and the result is fed to an integrator. The output of the integrator is sampled with an analog-to-digital converter. A full correlation can be collected by repeatedly adjusting the phase offset between the two signal branches and sampling the correlator output (Figure 2-4). The location of the various peaks in the full correlation indicates the location of impedance discontinuities such as open circuits, short circuits, and arcs (intermittent shorts). **Test data indicate that this test method can resolve faults in a noisy environment to within 1/10–1/100 of the length of a PN code chip on the cable, depending on the noise level, cable length, and type of cable.**

The operation of S/SSTDR depends on portions of the electrical signal being reflected at discontinuities in the characteristic impedance of the cable. The spread spectrum signal shown in Figure 2-3 is injected into the wires, and, as with TDR, the reflected signal is inverted for a short circuit and is right-side-up for an open circuit. The observed reflected signal is correlated with a copy of the injected signal. The shape of the correlation peaks is shown in Figure 2-4. In this figure, the modulating frequency is the same as the chip rate. Note that the side lobes in the correlation peak are sinusoids of the same amplitude as the off-peak autocorrelation of the ML code. This is due to the selected modulation frequency and synchronization. Use of a different modulation frequency or different synchronization will yield a different correlation pattern that may have higher amplitude side lobes (see Figure 2-5).

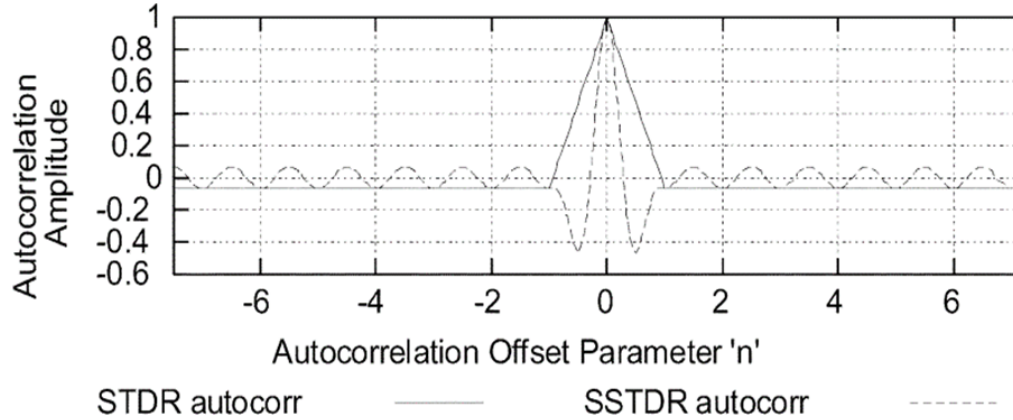


Figure 2-4. Autocorrelations of STDR and SSTDR signals from Figure 2-3.

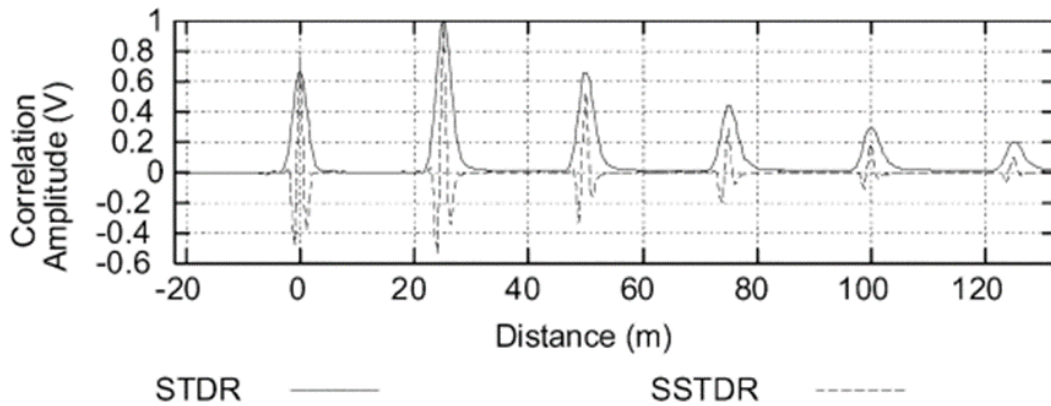


Figure 2-5. Correlator output for STDR and SSTDR tests on 75- $\Omega$  coax cable with an open circuit 23 m down the cable. Note the peak at zero (connection between the test system and cable), multiple reflections, and definitive shape of the correlation peaks.

The location of the peaks in the correlator output, in conjunction with an estimate of the velocity of propagation, indicates the distance to impedance discontinuities. Figure 2-5 shows normalized sample test data collected on a 75- $\Omega$  coax cable. The correlation peaks after 23 m are due to multiple reflections in the 23 m cable. The response for a paired conductor noncontrolled impedance (non-coax) cable is not as clean, which could be expected from the variation in impedance and subsequent small reflections, as well as minor variation in the velocity of propagation down the length of the cable. Figure 2-6 (a) and (b) show the STDR and SSTDR correlation responses measured on two 22 AWG wires in a loosely bundled set of 22 wires that is 9.9 m long. The wires snake in and out within the bundle and, although they are roughly parallel throughout, do not have even spacing throughout the bundle. The response is not as smooth as that seen in Figure 2-5 due to the multiple small reflections that occur within the uncontrolled impedance bundle. These multiple reflections, as well as the variations in the velocity of propagation, will reduce the accuracy of the method for uncontrolled impedance cables, as discussed below.

Figure 2-7 shows the STDR response for an 80 ft wire that is both short and open circuited on the end. Note that the first positive peak at 0 ft indicates that reflection is occurring where the high impedance circuit is attached to the wire. At the 80 ft location, a positive peak (for open) and negative peak (for short) indicate the end response. Hard faults (open and short circuits) can be located to within 3–5 inches on controlled impedance cables and within 6–8 inches on uncontrolled impedance cables. The S/SSTDR system can be used to locate small/quick/partial (~ 30% of a short circuit) intermittent results that can trip

an arc-fault-circuit-breaker. Such intermittent faults would be practically impossible to identify without the ability to monitor the live wire under operating conditions.

At least one vendor provides an S/SSTDR commercial system for live-wire aircraft fault detection (Chung Y. 2009). The system is based on a custom, application-specific integrated circuit that is small, lightweight, and inexpensive to manufacture in quantity. The system has been tested on live 60 Hz power lines, 400 Hz aircraft power lines, 28 V DC lines, and Mil Std 1,553 data lines.

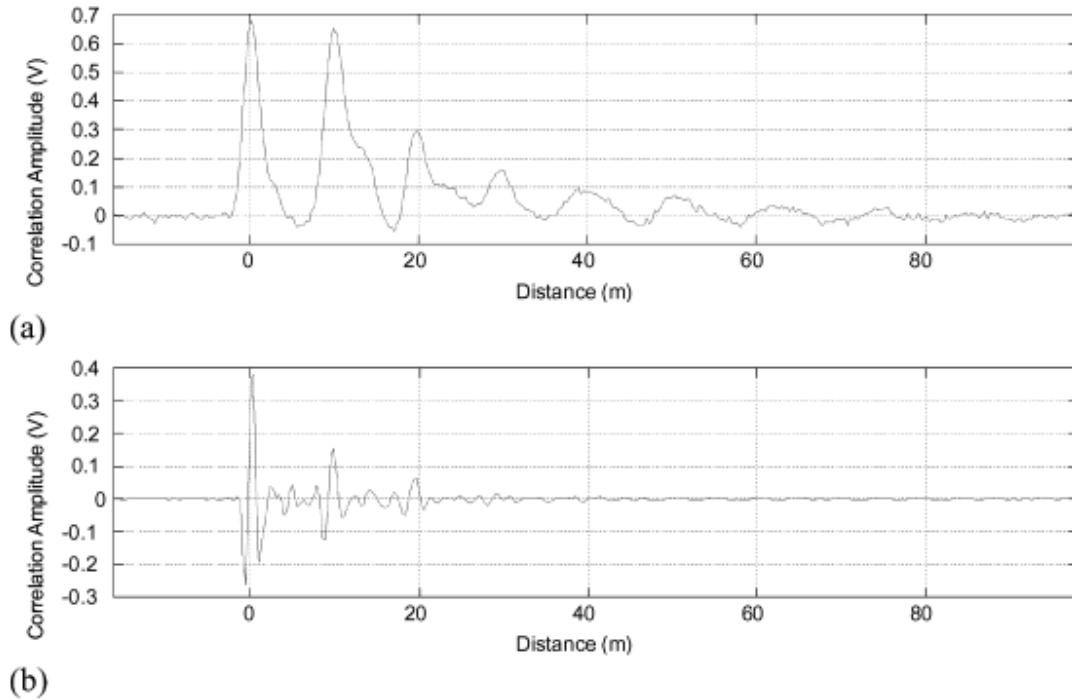


Figure 2-6. (a) STDR and (b) SSTDR correlation response for an open circuit measured on two 22 AWG loosely bundled wires that are 9.9 m long

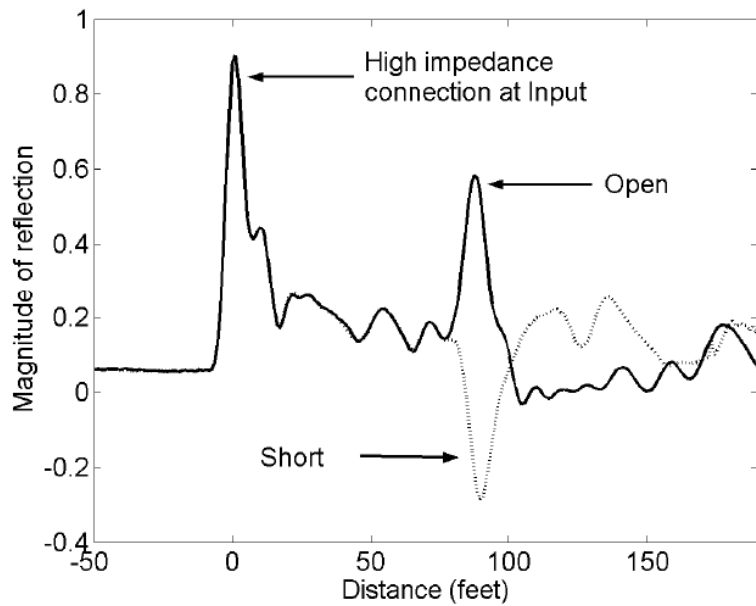


Figure 2-7. STDR response for an 80 ft wire with end open and short

### 2.1.3 Frequency Domain Reflectometry

Frequency domain reflectometry (FDR) is based on the interaction of electromagnetic waves with conductors and dielectric materials as the waves propagate along the cable. The technique uses the principles of transmission line theory to locate and quantify impedance changes in a cable circuit. These impedance changes can result from connections, faults in the conductors, or degradation in the cable polymer material (Mohr and Associates 2009) (Mohr and Associates 2010). For the FDR measurement, two conductors in the cable system are treated as a transmission line through which a LV, broad frequency waveform is propagated (Figure 2-8). As the broad frequency bandwidth signal and associated electromagnetic wave travels down the cable, a reflected wave is created at any impedance mismatch, and the reflected signal is recorded at each frequency to characterize the wave interaction with the conductors and surrounding dielectric materials. The captured frequency spectrum is transformed back to the time domain which is related to distance along the cable by the velocity of the wave propagation within the cable. Because the applied signal is LV, the test is nondestructive and poses no special safety concerns to operators.

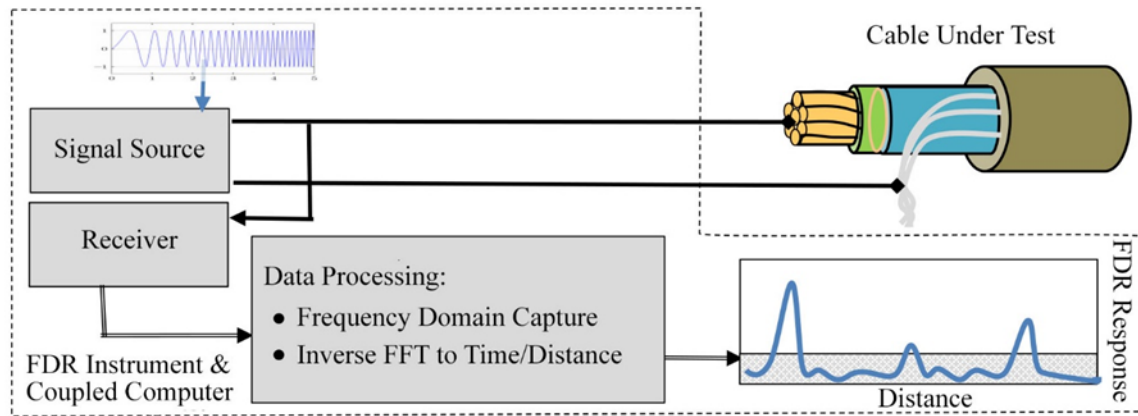


Figure 2-8. General FDR test uses 2 conductors to interrogate conductor and insulation-based cable impedance changes (Glass et al. 2016)

FDR measurements have demonstrated sensitivity to a number of cable parameters, some of which are useful to evaluate cable health and some of which are associated with the test and should be understood to distinguish them from cable health related issues. Some of these parameters (not an exhaustive list) are shown in Table 2-1 and many of these parameters were explored in (Glass et al. 2016).

Table 2-1. Cable/cable health related and cable test/environmental related FDR influence parameters

Cable/Cable health related FDR influence	Cable Test and environment FDR influence
Splices/Terminations	Temperature
Insulation geometry (cuts, gouges, pinches, thickness)	Proximity of different conductivity surfaces
Insulation permittivity change (from thermal or radiation)	Design – shielded, semi-conductor shield, twist, ...
Cable layout, bends/bend radius	Test frequency band width
Cable signal transmission velocity	FDR normalization and presentation
Cable signal attenuation	Specific FDR instrument
Cable length	Termination impedance (load connected or not)
Damage profile	

## 2.1.4 Comparison of reflectometry methods

A study performed in 2006 (Furse et al. 2006) compares several types of reflectometry systems focusing on aircraft wiring networks. Systems reviewed are summarized in Table 2-2.

Table 2-2. Comparison of reflectometry methods

Wire Fault Sensor	Accuracy (in)	Min length (in)	Estimated * Max length (ft)	Computational requirement **	Possibility of Network topology recognition
TDR (Megger 2020)	6-12	5	100+	Edge Identification	Yes
FDR (Furse et al. 2003) (Furse et al. 2005)	2	4 ***	50+ ***	Fast Fourier test (FFT); Peak Identification	Yes
S/SSTDR (Furse et al. 2005); (Smith 2003)	1	4	70+	Peak Identification	Yes
Capacitance or Capacitance/Inductance Sensor (Chung, Amarnath, and Furse 2009)	1	1	100+	Linear Curve Fit	No

\*Maximum length is based on maximum length the investigators have physically measured (typically 100 ft) and observed attenuation. The maximum length is dependent on wire type. Lossy wires have more attenuation and less measurable length than very low loss wires.

\*\*FFT requires significant computational power. Peak and edge identification can be minimal or can be more extensive if signal processing is used to improve results. Linear curve fit requires minimal computational power.

\*\*\*Furse tested and reported as shown. These cables were mostly aircraft LV cables. Other works (Glass et al. 2017) suggest industrial power cables must be at least 10–20 ft long and can be up to 3,000 ft or longer depending on the attenuation characteristics of the cable.

Capacitance/inductance methods are used in the simplest and least expensive sensors. Their range is large and, as a bulk measurement, they do not have limitations on minimum measurable length. Their accuracy and corresponding degradation sensitivity are comparable to or better than reflectometry method values. One significant limitation is that they cannot be used on live wires and they are not capable of locating faults on branched wiring networks, even with advanced computer processing of the data.

FDR methods are more expensive and more complex than capacitance and inductance sensors, but some can be used on branched wire networks. It is important to note that the exact minimum and maximum length and the expected accuracy and sensitivity to insulation degradation are dependent on the cable specific configuration as well as on test settings and the engineering design of the test configuration. For example, increasing the bandwidth of FDR or decreasing the rise time of a TDR pulse (which is equivalent to increasing its bandwidth) improves location accuracy. Increasing the length of time between rise and fall of the TDR pulse or increasing the number of frequency samples of the FDR increases the maximum range. Testable length is limited by the ability of the system to resolve two overlapping reflections. For TDR, decreasing the rise time of the pulse and the sampling interval helps. For FDR, removing the expected incident pulse using signal processing and increasing the resolution of the Fourier transform used to analyze the FDR data reduces the minimum measurable length. For all the reflectometry systems, it is possible to identify that there is a reflection within the minimum length, which is generally on the order of 2-ft, but not to determine accurately within this distance where the fault

occurs. In practice, this is not a severe limitation for aircraft, industrial, or home wiring, as knowing to within 1 or 2 ft where the fault has occurred is sufficient. Location accuracies of these methods are all comparable and are generally sufficient for both aircraft and industrial applications.

In a separate study contrasting FDR and TDR methods (Hashemian 2012), it was noted that FDR outperforms TDR in detecting problems within cable insulation materials such as a discontinuity, large cracks, or physical/mechanical damage. Normally this is a moot point as the two techniques are used complementarily in tandem to assess cable condition.

An important aspect of the reflectometry systems is the ability to run on live systems to detect intermittent faults. Currently, technicians would like to locate insulation chafes and frays that can result in intermittent faults. That is difficult or impossible with either TDR, FDR, or capacitance/inductance measurements. Locating conductor intermittent faults that are related to these conditions, however, can be done (Furse C. 2006). SSTDR reflectometry systems provide the best signal-to-noise ratio of all of the reflectometry systems and can therefore be used on low frequency (60 or 400 Hz) circuits as well as those carrying high speed data signals such as ethernet or (MIL 1553 1976). The next best signal-to-noise ratio is achieved by the STDR system, which is ideal for low frequency circuits and those in the kHz region. The STDR has less loss on the cable than SSTDR and is therefore able to test longer cables. FDR systems are limited to low frequency circuits, as they can interfere with the higher frequency lines. Even for the low frequency circuits, the signal-to-noise ratio of FDR is not as good as STDR. S/SSTDR systems are therefore the best for locating intermittent faults or for real-time testing of live circuits.

An important aspect of reflectometry systems for power distribution networks is applicability to branched circuits. Simple capacitance and inductance sensors are not capable of measuring branched networks so the system must be disconnected at each junction in order to individually test each line. This defeats the purpose of having a single-end test system. All the reflectometry systems have the potential to locate faults on branched networks since individual peaks or steps are seen in their response for each reflection point. Reflectometry responses from branched networks are often too complex to interpret by hand. The SWR and MSR systems have the most difficult (and in some cases have impossible) responses to evaluate, as they give peaks not only at junctions, ends of wires, and multiple reflection points, but they also provide all of the sums and differences of each of these points. TDR, S/SSTDR, and FDR are all similar in their responses and capability in this regard. Overlapping peaks/steps from reflections occurring very near the branches and multiple reflections that coincide with those at ends or junctions of branches are challenges for this method that can be addressed with a variety of signal processing techniques. Some aspects of networks will always be impossible to resolve with a single point measurement. For instance, when one of two identical circuit branches breaks, it is possible to tell how far away the break is, but it is possible to tell which branch is broken. When an open and short circuit occur at the same distance from the test system, the reflections cancel each other out and appear completely invisible. In cases such as these, multiple test points on the same system will be needed, which will in turn require the coordination and communication of data for analysis.

Smart imbedded test systems for wiring hold the promise of revolutionizing the way large wiring systems are designed and maintained. The ability to precisely identify and locate wiring faults remotely enables monitoring, diagnosis, control, and potentially even prognosis of degrading systems. Critical elements, including sensors that are small enough to be imbedded, that can locate faults on live systems and that can be used on branched networks are rapidly emerging and are showing excellent results.

Challenges for a fully embedded wiring test system remain. Not all network analysis can be completed from a single test point, which means that multiple sensors need to communicate in concert. The complexity of modern wiring systems means that there could potentially be thousands of distributed sensors in the highly lossy, high multipath communication environment of a building, an industrial power distribution network, or an airplane. Communication can be efficiently facilitated on the wires being tested, in some cases potentially with the same sensors that are used to test the wires, but if the wire breaks, then critical information would be lost. Where all arms of a wiring system are not continually

connected (for instance, data and power lines), a wireless communication system is needed. Modern communication protocols are optimized for high bandwidth data, but the data from these sensors (like data from most other sensors) is very limited, and the overhead from the communication protocol dominates the transmission. Thus, new protocols for large numbers of sensors sending small quantities of data are needed. This requires either integrating with an agreed common protocol or establishing a dedicated protocol for communication over wire or wirelessly that will not interfere with existing or future systems.

Another challenge for wiring systems is being able to handle the multiple wires within a bundle, either with multiplexers or with discrete (but small and inexpensive) sensors for each wire. S/SSTDR is capable of simultaneously testing each wire without causing electromagnetic interference with other wires, but other reflectometry systems could receive false reflections from wires other than the one they are testing. Multiplexers are available for high frequency signals and can be miniaturized, although there are issues of isolation and single points for failure within the system.

Another significant consideration is what to do with data processed from a large network of sensors. Methods to integrate location of faults within the wiring database that shows the location and routing of wires is very important. Ultimately, it would be ideal to have a system that shows the maintainer graphically where the fault occurred and how to fix it, much like a copy machine does when clearing a paper jam.

These test methods can be used for more than just locating faults on wiring systems. "Sacrificial" wires can be imbedded in concrete or other material, so that the wire breaks when damage occurs to the structure. The location of damage could be inferred by measuring the wire. Corrosion may also be detectable in this way. Many of the methods described here have parallels in fiber optics, which opens new opportunities both for testing of wire or fiber optic systems and for sacrificial wire or optical fibers.

Aging wiring is a longstanding problem, and the proliferation of electronic systems within society is further propagating that problem. Test methods to locate faults, or to locate early intermittent predecessors to catastrophic faults, can dramatically decrease the maintenance cost and time burdens as well as improve safety. Handheld systems and permanently installed systems suitable for live-wire monitoring are emerging. These methods promise a shift in electrical maintenance and open opportunities for robust and inexpensive imbedded structural sensors that have not previously existed.

## 2.2 Partial Discharge Detection with Cable as Waveguide

Partial discharge (PD) in a cable refers to a pulse-current that occurs when the cable insulation fails to withstand an electrical field applied to it. Causes include workmanship of splices or connector terminations, defective materials, contamination, material aging, and progression of water or electrical treeing. A PD pulse is relatively short (< 100 ns) and occurs when the voltage stress exceeds the insulation breakdown strength. Typical offline PD testing (Figure 2-9) uses a very low frequency stress applied to the central conductors. Voltage is ramped up until discharges are detected or until a designated maximum test voltage (typically 1.5-2.5 \* operating voltage or  $U_0$ ) is reached. For online testing, (Figure 2-10) the discharge is normally sensed by coupling to the shield or ground straps and takes advantage of the closed circuit consisting of the conductor, the coupling across the insulation, and the shield. Online testing only challenges the system at the normal operating voltage. The PD is a relatively low-energy, short-duration pulse that can be detected with electrical monitoring and test instrumentation and in many cases also by ultrasonic emissions sensed with directional microphones, fiber optics, or sensors directly on the cable. If not addressed, the discharge spark erodes the insulation via heat and ionization and can ultimately lead to a catastrophic failure (HV Diagnostic Technologies 2019).

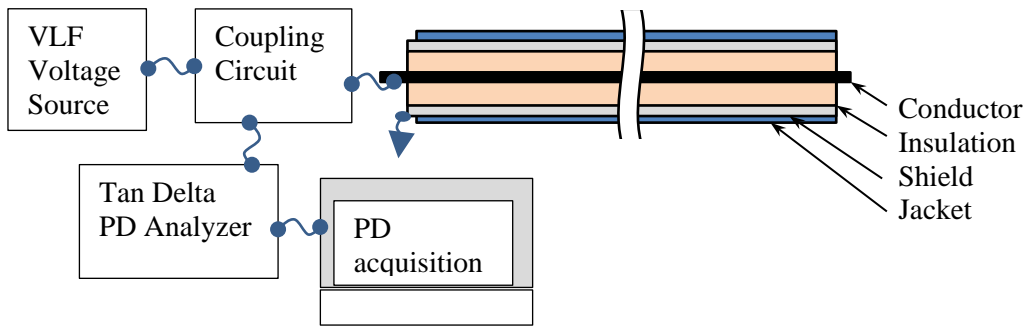


Figure 2-9. Typical offline tan delta and partial discharge connection configuration. VLF – very low frequency

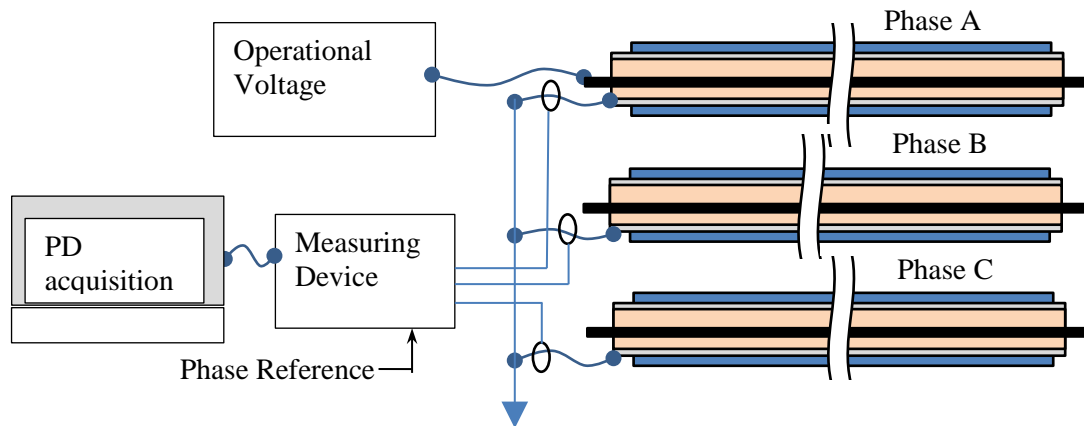


Figure 2-10. Typical online partial discharge monitoring configuration

The PD measurement is a suitable method to detect and localize imperfections in a MV or HV insulation system and provides a procedure for quality assurance of electrical equipment. Detection and location of PD can be determined by several non-electrical methods as listed below and can be useful to identify and locate PD without connecting a special electrical unit.

- Aural or auditory perception of the characteristic corona buzz
- Contact microphone
- Heat detection (fiber, thermocouples, or infrared)
- Light detection (with translucent dielectrics or on visible PD surfaces, particularly for ultraviolet [UV] wavelengths)

Electrical methods for PD detection, however, are far more sensitive and offer a quantitative approach to characterizing cable damage (Chakraborty 2017).

In an energized insulation system containing insulation defects, the voltage appearing across the defects will follow the waveform of the applied voltage on the cable. If the electric field at the defect is

greater than the breakdown strength of the insulation at that location, a partial discharge will occur. The partial discharge starts as soon as the applied voltage exceeds the PD initiation voltage and stops when the applied voltage drops below the extinction voltage. This sequence can also be portrayed using an equivalent circuit diagram as shown below (Figure 2-11).

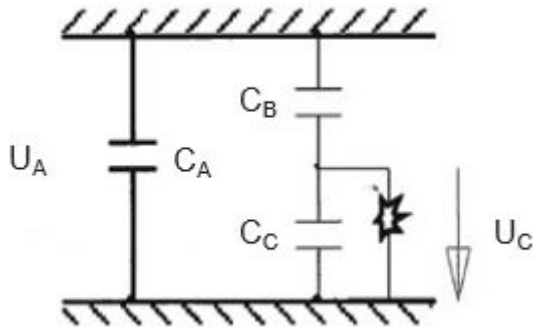


Figure 2-11. PD equivalent circuit with a void containing PD

The voltage appearing across a cavity  $U_C$  by applying an alternating voltage  $U_A$  to the device under test (DUT) is given by:

$$U_C = U_A * \frac{C_B}{C_B + C_C}$$

where  $C_A$  is the capacitance of the DUT,  $C_B$  is the capacitance of the healthy insulation in series to the cavity, and  $C_C$  is the capacitance of the gas within the cavity. This also allows the apparent charge  $q_A$  to be measured in picocoulombs (pC), given as  $q_A = C_B * \Delta U_C = C_A * \Delta U_A$ . PD signals occur in the nanosecond time scale so that the discharges appear as pulse like currents that can be superimposed over one cycle of the AC waveform (e.g. 16.7 ms for 60 Hz). This is also known as a phase-resolved PD pattern (Figure 2-12) (Konig and Rao 1993).

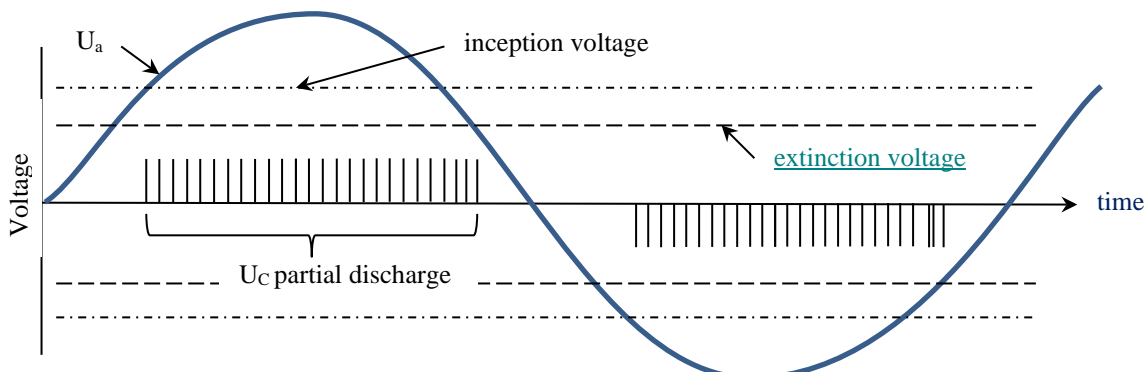


Figure 2-12 Graphical representation of voltage appearing across device under test showing PD beginning when  $U_A$  exceeds inception voltage and ending when it drops below extinction voltage.

The characteristic PD signatures can be a useful tool in determining what type of defect is present in the insulation system being tested. The pulses tend to appear in pulse trains with polarity similar to the applied AC voltage. In general, the number of discharges will increase in frequency with applied test voltage. The amplitude of the PD signals will tend to remain constant in cavities within solid insulation

due to space limitations. On the other hand, PD amplitudes will increase with increasing applied voltage in liquids or during tracking discharges in air where there is less restricted volume of gas for the streamers (visible breakdown trails) to grow. Most discharges will superimpose on the higher absolute value voltage of the AC sinewave.

Data obtained through PD testing and monitoring can provide critical information on the quality of insulation and its impact on overall equipment health. PD activity may be present well in advance of insulation failure and, if monitored online over time, can support proactive asset management to prevent a catastrophic failure.

Online PD testing is performed while the equipment is energized at normal operating voltages. The testing is conducted during real operating conditions, under typical temperature, voltage stresses, and vibration levels. It is a nondestructive test (NDT) and does not use overvoltages that could adversely affect the equipment. Online PD testing is inexpensive compared to offline testing that requires interruption of service and production. For critical facilities with continuous operation, an online PD monitor provides continuous protection without requiring operational interruption to test the circuit. One downside of online monitors is that there is no flexibility to challenge the system with higher-than-normal operating voltages to increase the likelihood of producing PD to detect early stage insulation degradation.

Permanently-mounted sensors for hard-to-access areas or areas that pose a safety concern can be used for periodic online PD detection. These sensors remain on the equipment for online access and diagnostic information. Often, these sensors must be installed during an outage or plant downtime. Once installed, no further outage or disruptions are required for online testing.

The benefits of online PD field measurements include:

- It is truly a predictive test, indicating insulation degradation in advance of the failure
- It is a non-intrusive test, requiring no interruption of service and is performed under normal operating voltage and load
- It is a nondestructive test: it does not test to failure or adversely affect equipment under test
- It need not use any overvoltage, thereby not exposing the tested equipment to higher voltage stresses than those encountered under normal operating conditions
- Trending can be accomplished by storing results to allow comparison with future tests
- In many instances the site of PD occurrence can be located within the test object, so that the localized problem can be repaired. Offline PD testing however may more readily locate the PD site
- The cost to perform a PD survey is relatively inexpensive compared with offline testing, allowing frequent periodic or continuous permanently mounted surveys to be performed economically at most facilities

Offline PD testing offers significant advantage over other technologies because of its ability to measure the response of the cable system to a specific stress level and predict its future performance without causing a fault. Offline testing is also known for its ability to better pinpoint the defect location on field-aged equipment compared to other techniques, enabling the asset manager to accurately plan for maintenance repair. The challenge with offline testing is that equipment must be taken offline and out of service. Offline testing is also commonly used in acceptance testing on newly installed cables. PD can be detected in branched cable systems but location efforts are significantly complicated by branching.

Table 2-3 provides a list of example companies and products offering various levels of offline and online PD monitoring using the cable as a waveguide.

Table 2-3. Companies and products for electrical, thermal, IR, UV, and acoustic PD monitoring

<b>Company/Product</b>	<b>Notes/Features</b>
<b>HV Technologies/ Liona</b>	Offers online, offline, and tan delta test units and service. The Liona model is for online cable assessment of HV and MV cables. Features ultrasound probe for defect location.
<b>DMV/GL Smart Cable Guard (Norway and Germany)</b>	Focuses on MV cable clamp-on continuous monitoring with advanced noise reduction software.
<b>Omicron/Moncablo</b>	Targets HV cables. Inductive power supply where LV is unavailable. Communicates via fiber optic or ethernet. Sends e-mail to designated recipient if PD exceeds threshold.
<b>Omicron/PDL 650</b>	Features up to four channels of acoustic sensor designed to “listen” for PD in transformers, motors, and other components.
<b>IRIS Systems/SONUS</b>	Specifically designed for PD airborne acoustic emission (AE) detection on MV and HV switchgear. This is a small phone-linked system with headphones to help with direction sensitivity and loud industrial setting noise immunity that generates the report on the phone.
<b>Dobel/DFA300</b>	This surveying tool for PD detection combines radio frequency interference and AE.
<b>FLIR/Si124</b>	Infrared acoustic imaging camera that can detect partial discharge from HV electrical systems.
<b>SONEL Test &amp; Measurement/UV260</b>	Filters pass UV light to detect and locate in-air visible corona discharge.

## 2.3 Fiber Optic Temperature and Acoustic Measurements

### 2.3.1 Bragg Grating Measurements

The simplest form of fiber optic sensor measurement is to examine the reflection from a discrete Bragg grating as shown in Figure 2-13. The spacing between Bragg sensors are customized during fiber fabrication. A laser light pulse is injected into the fiber end and the instrument senses the specific light wavelength corresponding to the Bragg sensor grating spacing. Any wavelength shift compared to the reference signal is indicative of a grating spacing change corresponding to strain or temperature change. This technology has been practiced since the late 1970s and permits a sensitivity of  $\pm 1$  part per million, which corresponds to a temperature sensitivity of  $> 0.1^\circ\text{C}$  (Allil et al. 2013) and strain sensitivity of  $> 0.7 \text{ me}$  (Campanella et al. 2018).

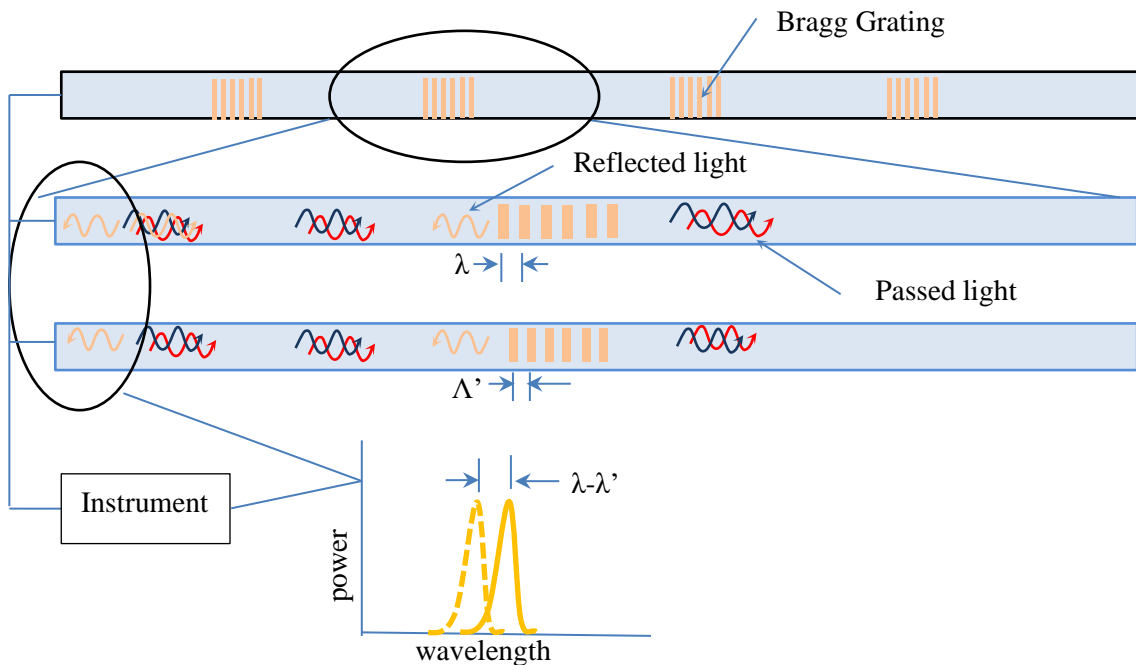


Figure 2-13. Change in Bragg grating distance can be proportional to change in temperature or strain

### 2.3.2 Distributed Optical Fiber Sensors

Generally, Bragg sensors provide a stronger signal and can be made to work over longer distances than many electrical measurements, but spatial resolution is limited by the Bragg spacing (typically a few feet or less). Distributed optical fiber sensors do not rely on discrete Bragg gratings to reflect the laser pulse. Rather, reflections are created by back-scattering from imperfections in the fiber or from light reflections from the cladding back into the core. Three scattering mechanisms (listed in order of signal magnitude) can be exploited to realize a distributed fiber sensor: Rayleigh, Brillouin, and Raman (Rajeev et al. 2013). Rayleigh scattering is an elastic phenomenon (like Fresnel reflection) while Brillouin and Raman scattering are based on inelastic (nonlinear) scattering. The three spectral modes can be used to sense various parameters within the fiber (Figure 2-14). Distributed optical fiber sensors are used in oil and gas exploration, pipeline monitoring, intrusion monitoring of facilities, and state-of-health monitoring of machinery and buildings. The focus for the operation of Rayleigh scattering-based sensors is detection of strain along the longitudinal axis of the fiber as manifested in changes in scattering due to fiber strain along the fiber length. However, distributed temperature sensing is generally better served by Brillouin or Raman scattering approaches which are more sensitive to temperature than strain. Signal strength for

these is reduced, however, relative to Rayleigh elastic scattering. Some alternate approaches to measuring temperature using Rayleigh methods (Nikitin et al. 2018) may also be applicable for longer fibers.

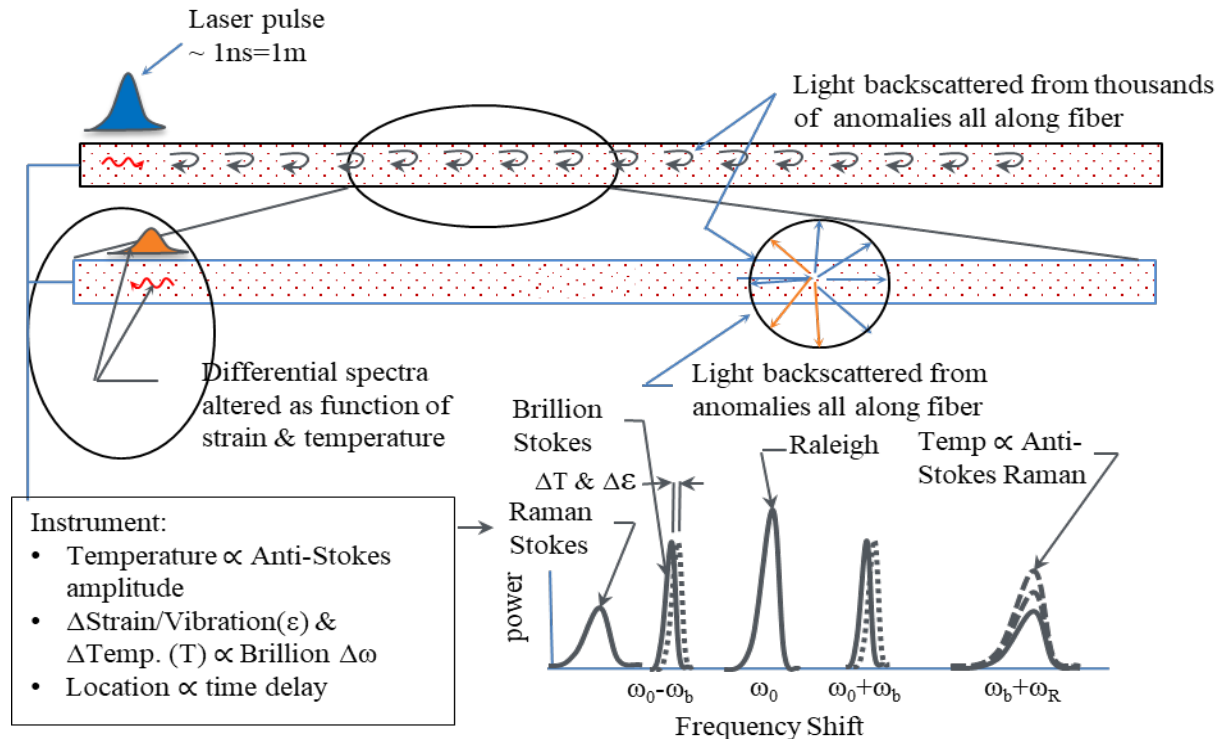


Figure 2-14. Distributed temperature and strain fiber optic sensing based on changes in reflections from anomalies along the full length of the fiber as indicated by Raman and Brillouin peaks. Location information is based on reflection time delay.

These and other methods of distributed sensing are investigated to gain an understanding of each technique, its strengths and weaknesses, and potential application. An envisioned state-of-health monitoring (SHM) concept is that a single optical fiber could be wound around multiple components and a single laser-based instrument would acquire localized strain and temperature measurements of each component.

### 2.3.3 Rayleigh Scattering

The theoretical description of the measurement of strain using Rayleigh scattering produced by an optical fiber is covered in detail by (Froggatt and Moore 1998). Rayleigh scattering is due to random fluctuations in the index of refraction of the fiber core. This phenomenon can be modeled as a one-dimensional change in refractive index as a function of distance (Rogers and Handerek 1992). Froggatt and Moore (1998) show that Rayleigh scattering can be modeled as a Bragg grating with random variations of amplitude and phase along the grating length. They demonstrate that this approach is useful as it is capable of very high stress resolution of 10 ppm over a 30 cm length of fiber with a spatial resolution of approximately 0.6 cm.

Froggatt and Moore (1998) showed that the complex amplitude of the backscattered field from a random fluctuation as a function of distance is the Fourier transform of the refractivity evaluated at twice the spatial frequency of the excitation field. Strain is therefore determined by measuring the shift in the Rayleigh scatter spectra. Since the spectra are random in nature, the spectrum of the same section measured with no strain applied must be performed to identify the shift in the strained spectrum, and hence, degree of strain.

This approach is implemented in the products offered by Luna Innovations, which specializes in near-field, high-resolution strain sensing. More conventional Rayleigh scattering-based sensors such as those offered by OptaSense or Silixa work by injecting a narrow pulse of laser light into a single mode fiber. The change in the index of refraction and length of the fiber due to thermal, acoustic, or seismic signals are measured using coherent optical time domain reflectometry (COTDR) and measuring the amplitude and phase of the backscattered pulses (Duckworth and Ku 2013). In COTDR a portion of the interrogation pulse is split off and used as a local oscillator to interfere with the backscattered light (Iida et al. 2012). This is shown schematically in Figure 2-15.

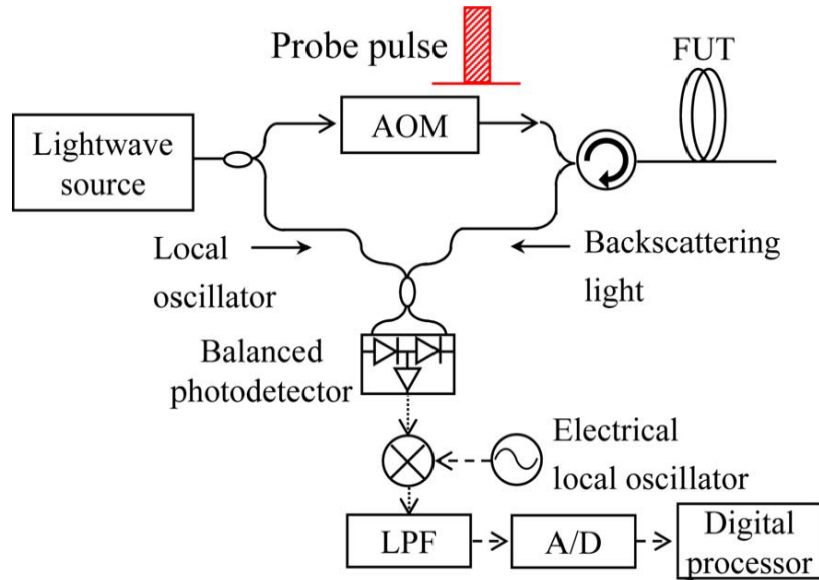


Figure 2-15. A notional COTDR system showing the source, modulator, local oscillator, backscattered signal, and detector (from Iida et al. 2012)

### 2.3.4 Brillouin Scattering

Brillouin scattering is extensively covered in a review article by (Galindez-Jamioy and López-Higuer 2012) and occurs when optical power exceeds the power threshold needed to induce nonlinear phenomena. The scattering depends strongly on environmental factors such as stress and temperature. Incident light generates acoustic waves by the electro-constriction effect, which induces a periodic modulation of the refractive index that causes light to backscatter, similar to a Bragg grating. This backscattered light is downshifted due to the Doppler shift with the grating moving at the acoustic velocity in the fiber.

Stimulated Brillouin scattering is a pump/probe technique and is a process by which scattering is enhanced when the difference in frequency between the pump and continuous wave probe signal is equal to the Brillouin shift and both signals are counter propagating in the fiber. Brillouin frequency has a linear dependence on applied strain  $\epsilon$  and temperature variation ( $\Delta T$ ) (within restricted tolerance ranges). The Brillouin frequency shift is 10–11 GHz at 1550 nm and can be localized in the fiber by using either time or frequency domain methods.

Brillouin sensors may be either spontaneous or stimulated. Spontaneous sensors use only incident laser light launched with no additional stimulus on photon generation. Coherent detection can give greater dynamic range to measure temperature and strain, but its drawbacks are:

- Incident laser power must be restricted to avoid nonlinear effects
- The backscattered signal is weak (weaker than Rayleigh scattering)
- The round-trip loss in the fiber is significant at 0.4 dB/km, which limits its effective range to less than 50 km

Spontaneous Brillouin scattering can be measured using Brillouin optical time-domain analysis, Brillouin optical correlation-domain reflectometry, and measurement of the Landau-Placzek ratio. The Landau-Placzek ratio is the ratio of Rayleigh to Brillouin light, which only depends on temperature and is one method to isolate temperature from strain in Brillouin-based measurements.

Stimulated Brillouin scattering provides enhanced signal return with increased measurement complexity and the requirement of a fiber loop arrangement to facilitate location of the pump and probe lasers and signal processing apparatus. Omnisens offers the distributed temperature test (DITEST) stimulated Brillouin scattering system that provides both distributed temperature as well as strain measurements and has been in use since 2003 (Nikles et al. 2004) (Nikles 2009).

### 2.3.5 Raman Scattering

Early efforts at distributed temperature sensing were first reported by (Dakin et al. 1985) using inelastic scattering arising from laser light being scattered at frequencies equal to the vibrational frequency of the molecules involved. In this scenario the scattered light is shifted both to lower frequencies (Stokes) and higher frequencies (anti-Stokes). For fused silica,  $\Delta f$  is 13.2 THz or  $440 \text{ cm}^{-1}$  (Farahani and Gogolla 1999). The temperature sensitivity of the Raman scattered light is determined by the Maxwell-Boltzmann energy partition between the various vibrational states of the vitreous macromolecule of the glass fiber. By measuring the ratio of the Stokes to the anti-Stokes line, absolute temperature measurements can be taken using the expression below.

$$R(T) = \left(\frac{\lambda_S}{\lambda_A}\right)^4 e^{-\frac{hc\tilde{v}}{kT}} \quad (1)$$

In equation 1,  $\tilde{v}$  is the wavenumber separation with respect to the pump wavelength,  $h$  is Planck's constant,  $k$  is Boltzmann's constant, and  $T$  is the absolute temperature of the fiber core where the light is received. While distributed temperature sensing using Raman scattering may be of interest in building SHM, Raman scattered light is the weakest scattered signal and is thus the most challenging to make work over long stretches of optical fiber.

### 2.3.6 Commercial Fiber Optic Instrumentation

Table 2-4 lists the several companies that offer commercial off-the-shelf systems. Not unexpectedly, little open source information is available for many of these sensors. OptaSense and Silixa sensors provided the most detailed information on performance. Luna Innovations is included but its technology is based on a frequency modulated continuous wave (FMCW) approach and range is limited by the chirp achievable with the laser. Luna is focused on measuring strain in manufacturing, building, and SHM scenarios, with impressive spatial resolution but insufficient range for applications such as seismic or long-distance temperature monitoring. Several vendors offer custom fiber geometries for specialized measurements including imbedded cable monitoring. OZ optics (Optics 2016), AP sensing (AP Sensing 2020b), and Marmon (Marmon 2019) are more commercially focused on cable applications.

Table 2-4. Selection (not comprehensive) of companies offering commercial off-the-shelf fiber optic instrumentation systems

Vendor	Model	Technology	Range	Temperature Resolution	Spatial Resolution	Sample Frequency	Strain sensitivity	Notes
Silixa	iDAS	Raman & Brillouin Scattering	125 km	0.5°C	1 m	1 kHz	10 $\mu\epsilon$	
OptaSense	ODH4	Rayleigh Scattering	40 km		1.3 m	100 kHz		Primarily for pipeline acoustic leaks & seismic. (Optasense 2016)
Luna Innovations	ODiSI	Rayleigh Scattering (FMCW excitation)	50 m		1.28 mm	2.5 Hz		Optimized for near-field, high sensitivity strain measurements
Omnisens	DITEST	Stimulated Brillouin Scattering	50 km	0.1 m	0.5 m			Needs counter propagating pump
OZ Optics	Foresight	Brillouin Scattering	100 km	0.5 cm	1 m	1 kHz	25 dB	Can be operated either as looped or single-ended
AP Sensing	DTS N45	Raman Scattering	Several km to 70 km		0.5 m	1 Hz		Power cable; (AP Sensing 2020a) (AP Sensing 2020b)
Marmon Sensor	Power Cable Monitoring	Brillouin Scattering		+/- 1°C from 10 to +60°C	1 m	0.5-15 minutes		More focused on temperature than noise

While one advantage touted for distributed fiber optic sensing is the ability to use common telecom cables, either already installed or custom, many environments such as in oil and gas exploration are hostile to typical photonic components (> 200 °C temperature and 15,000 psi). Specialized cables, while perhaps designed to enhance desired signals, must be hardened to the hazards unique to the application environment. Omnisens offers optimized cables that are designed to enhance the transfer of strain to the fiber where it can be sensed. Typical fiber optic armored cables are generally designed in such a way as to prevent strain on the cable, typically with a Kevlar sheath, so that if a cable is pulled the force is transferred to the sheath and not the glass fiber.

One research technique to optimize a fiber optic cable for sensing both axial and transverse forces is fiber shaping (such as a helically shaped fiber). This method is more sensitive to detect vector components non-parallel to the axial direction of the fiber (Lumens 2014) (Lumens et al. 2013) (Figure 2-16 and Figure 2-17 below). Cable solutions involve mass-spring systems and an inertial member to induce axial strain in the fiber caused by broadside motion.

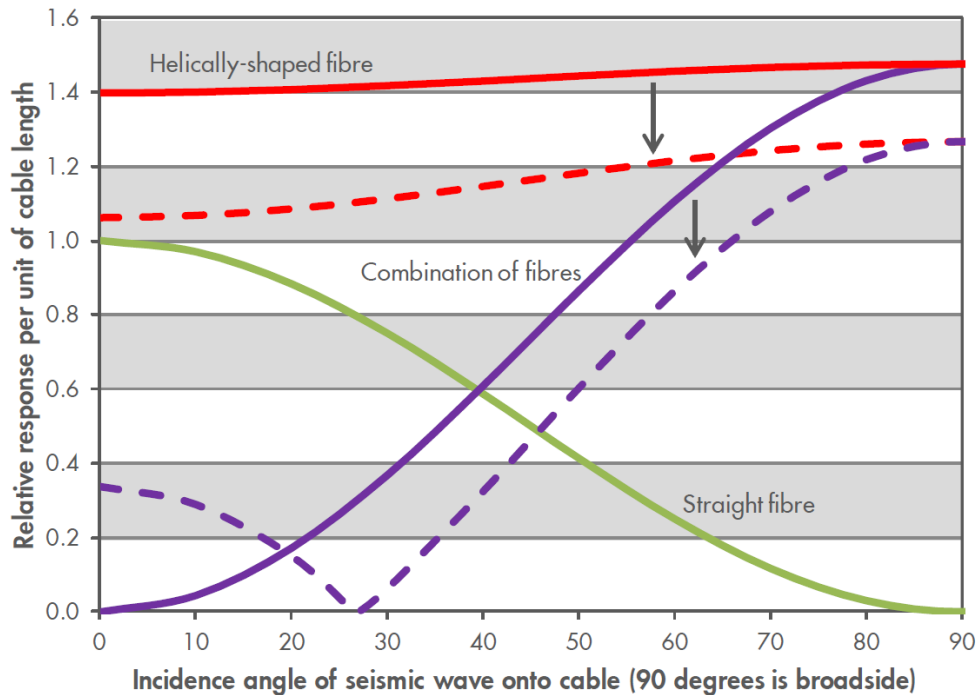


Figure 2-16. Fiber shaping signal amplitude as a function of angle of incidence  $\theta$  for a cable with a straight fiber (green), a helical fiber (red) and a linear combination of helical plus straight for two ground conditions (Lumens et al. 2013). For soil harder than that encountered, the response would follow the dotted lines. All curves normalized based on the response at  $\theta = 0^\circ$  of a cable with a straight fiber (Lumens 2014) (Lumens et al 2013).

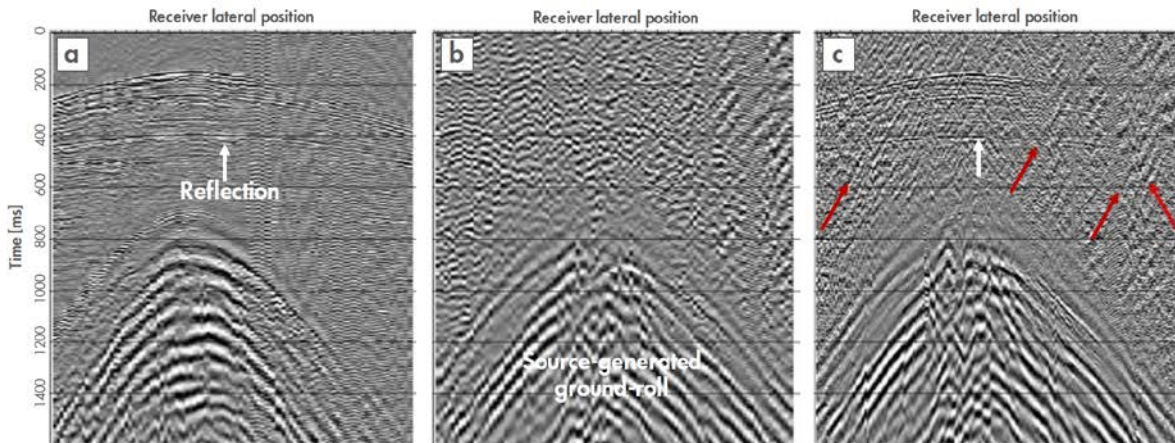


Figure 2-17. Shot record of three located sensor systems: (a) vertical accelerometer, (b) a straight fiber, (c) a shaped fiber. White arrows point to reflected energy, not present on the straight fiber plot, and the red arrows in the shaped fiber plot point to ground roll from ambient noise sources (Lumens 2014)

## 2.4 IDC Sensors for Online Monitoring

IDC sensors are characterized as external jacket/insulation measurements. First demonstrated in the context of planar surfaces (Igreja and Dias 2004) (Mamishev et al. 2004) (Zaretsky, Mouayad, and Melcher 1988), IDCs are designed for use on a single surface of a sample or test piece rather than by sandwiching a sample between two electrodes. The ability to apply a sensor to a single surface of a sample is often advantageous in online monitoring where other surfaces are inaccessible.

Much of the initial work on wire and cable polymer monitoring focused on the development of curved clamp sensors through which the capacitor electrodes were applied to the surface of a wire or cable by means of mechanical pressure. In early work, curved electrodes were applied to insulated wiring (Chen T. 2012) for the purpose of measuring the permittivity of the insulating layer coating the conductive core. The capacitive sensor consisted of two identical curved patch electrodes exterior to and coaxial with the cylindrical polymer test piece. The permittivity of the polymer was determined from measurements of capacitance matched to the predicted capacitance of a physics-based model of the sensor and cable system. To demonstrate the effectiveness of the sensor, measurements of capacitance were made on aircraft wires and the permittivity of the insulation inferred. A significant change in permittivity was observed for thermally degraded wires. With the goal of increasing signal-to-noise ratio, (Sheldon and Bowler 2014) invented an IDC clamp sensor and applied it successfully for measuring the permittivity of wire insulation materials. A handheld prototype sensor suitable for clamping to aircraft wire was designed (Figure 2-18) and measurements of capacitance were made on M5086 aircraft wire. This wire consists of tin-coated copper strands insulated with flexible polyvinyl chloride (PVC), a glass fiber braid, and finally coated with Nylon 6. After exposure to various common aircraft fluids (cleaner, deicer, distilled water, hydraulic fluid, isopropanol, and jet fuel), the measurements showed significant changes in measured capacitance, correlating well with the results of accelerated aging experiments on pure Nylon 6.

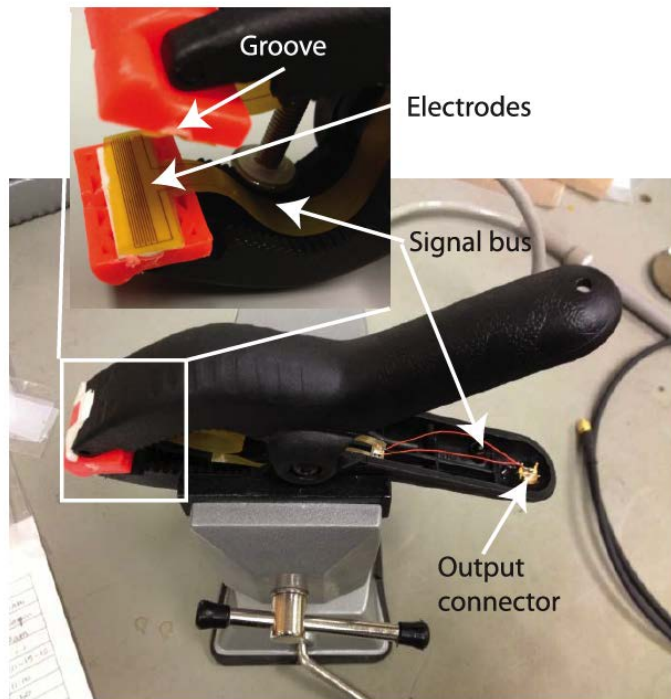


Figure 2-18. Plastic spring-loaded clamp sensor with inset showing detail of the jaws and interdigital electrodes attached to both orange jaws (Sheldon and Bowler, 2014)

Further work showed that the sensor was capable of measuring dissipation factor (also known as dielectric loss tangent or tan delta) that correlated closely with measured indenter modulus (IM) made on cables insulated with flame-retardant ethylene–propylene rubber (EPR) (Arvia, Sheldon, and Bowler 2014). Cable samples were prepared by accelerated aging in various thermal and ionizing radiation environments. The measured IM and dielectric loss tangent showed a high degree of correlation, whereas the dielectric measurements were found to be easier and quicker to perform than the indenter measurements.

(Glass, Al-Imran, et al. 2019) used an inexpensive capacitance-to-digital converter to explore different configurations of the IDC, particularly including with and without copper backing/shielding. Sensors with copper backing/shielding were noted to have a deeper penetration depth. The notion of an inexpensive wireless transmitter to monitor insulation condition was further considered by (Imran et al. 2020) (Figure 2-19 and Figure 2-20) where power harvesting wireless transmitters could be widely distributed throughout an NPP to continuously monitor the health of critical cables.

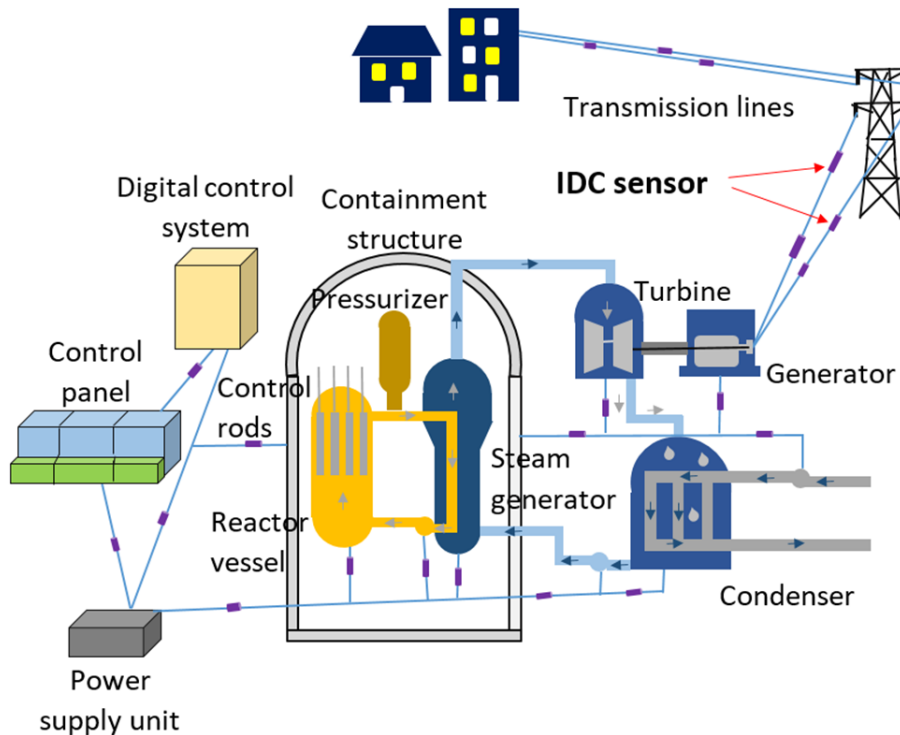


Figure 2-19. Illustration of possible NPP configuration with numerous surface mount IDC sensors deployed for continuous monitoring of cable health (from Al-Imran et al 2020)

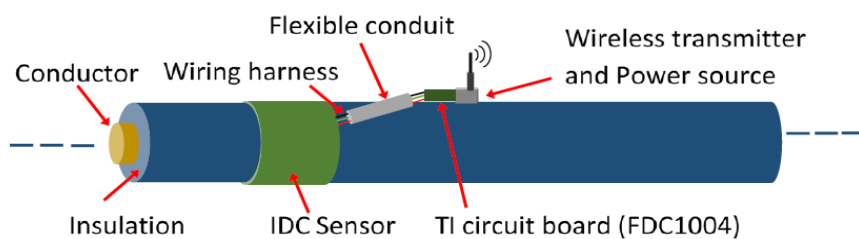


Figure 2-20. Illustration of patch IDC sensor with auxiliary components necessary for a continuous cable health monitoring system (from Al-Imran et al 2020)

A capacitance sensor is capable of sensing changes in the dielectric properties of a material. The presenting dielectric properties of a material derive from a combination of various polarization mechanisms that may be present in the material. In polymer systems, common polarization mechanisms include:

- a) atomic polarization due to relative displacement of the atomic nucleus and electron cloud upon application of an electric field, present in all materials
- b) dipolar polarization due to rotation of permanent dipole moments upon application of an electric field, these may exist along a polymer backbone or inside groups attached to the main polymer chain, for example
- c) hopping of charge carriers between localized states, this may be enhanced as a polymer ages if free charges are released in that process
- d) interfacial polarization whereby mobile charges become trapped at interfaces as they migrate under the influence of an applied electric field, common in semi-crystalline polymers at the boundary between the amorphous and crystalline phases, for example.

As a polymer ages, the strength of these polarization mechanisms may increase or decline depending upon the way in which the aging is induced. In addition to changes in polarization, a dielectric may become more conductive as it ages due to charge injection or enhanced mobility of impurities, among other possibilities. A change in conductivity is manifested as a change in the imaginary part of the permittivity  $\varepsilon$  defined as follows:

$$D = \varepsilon E$$

where  $D$  is electric displacement and  $E$  is electric field. The permittivity  $\varepsilon$  captures the electrical response of the material to  $E$  since:

$$D = E + \chi E = (1 + \chi)E = \varepsilon E$$

and  $\chi$  is the electric susceptibility of the material. The permittivity is a complex number and is generally dependent on frequency,  $f$ :

$$D(f) = \varepsilon(f)E = [\varepsilon'(f) - j\varepsilon''(f)]E$$

For the reasons listed above, the permittivity of a polymeric material is frequency dependent, tending to decline as frequency increases (Figure 2-21)

because the ability of each electric dipole to contribute to the overall permittivity relies upon its ability to rotate or otherwise respond to the changing direction of the applied alternating electric field. Taking dipolar polarization in a polymer as an example, the ability of a permanent dipole to contribute to the overall polarization of the material relies upon its ability to rotate within its local environment. The bulkier a dipolar side group is, for example, the lower will be the frequency above which it no longer contributes to the overall polarization of the material. This frequency is known as the relaxation frequency. The real part of the permittivity of the material transitions to a lower value through this frequency whereas the imaginary part of the permittivity peaks there. Figure

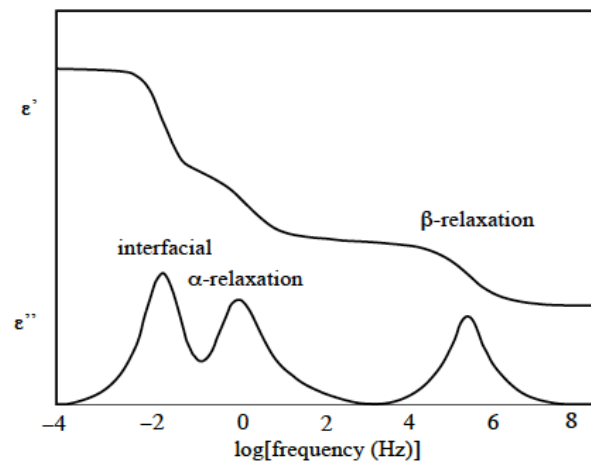


Figure 2-21. Schematic presentation of frequency dependence of permittivity for typical relaxation modes in polymers (Bowler and Liu, 2015)

2-21 illustrates two dipolar relaxations in a polymer; the  $\alpha$ -relaxation is associated with motions of the polymer backbone whereas the  $\beta$  relaxation is associated with the motion of molecular side groups. More detail is provided in (Bowler and Liu 2015).

The IDC sensor presented in Figure 2-18 was tested on wires insulated with flame-resistant (FR) EPR of three colors aged at 80, 90 or 100 °C and a radiation level of 100 Gy/h for exposure times between 1,177–5,781 h. Comparing IM and tensile elongation-at-break (EAB) data taken on the same samples, results showed that capacitance C and dissipation factor D measured at either 1 kHz or 1 MHz correlated more strongly with IM (with correlation magnitudes greater than 0.9) than the correlations between IM and EAB (Bowler and Liu 2015).

Frequently, the external jacket of a cable is significantly degraded while the underlying insulation is not due to differences in the susceptibility to degradation of the materials used in the two functions. Program researchers at PNNL and ISU extended the IDC test to evaluate insulation through an intact jacket (Glass III et al. 2018). This measurement is only applicable to cables without shield, foil, or semiconductor isolation between the IDC sensor and the insulation to be tested. This constraint still leaves a large population of cables that can be tested with the IDC sensor. The sensor configuration with and without a jacket is shown in Figure 2-22.

A set of EPR insulated cables with a chlorinated polyethylene (CPE) jacket were thermally aged at 140°C to produce a range of age-related permittivity values for IDC capacitance and dissipation factor measurements. By exploiting different depths of field of the measurement with wide and narrow sensor tine spacing, insulation condition can be inferred through a jacket. The wide-tine sensor depth of field extends beyond the jacket and is sensitive to permittivity of both the insulation and the jacket. The narrow-tined sensor with its shallower depth of field is primarily sensitive only to the jacket permittivity. The relative depths of field are shown by finite element modeling in Figure 2-23. The ability of dual (wide and narrow gap tined) IDC sensors to assess insulation conditions was demonstrated using the samples shown in Figure 2-24, where a series of artificially aged EPR cables with a PVC jacket are picture. On half of

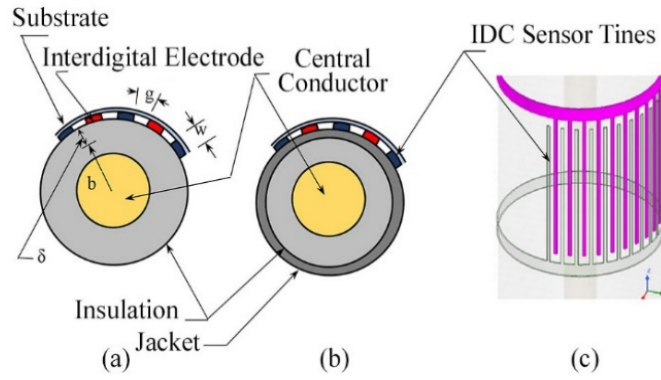


Figure 2-22. (a) Unjacketed cable cross section with IDC, (b) jacketed cross section, (c) orthogonal view of IDC (Glass III et al. 2018)

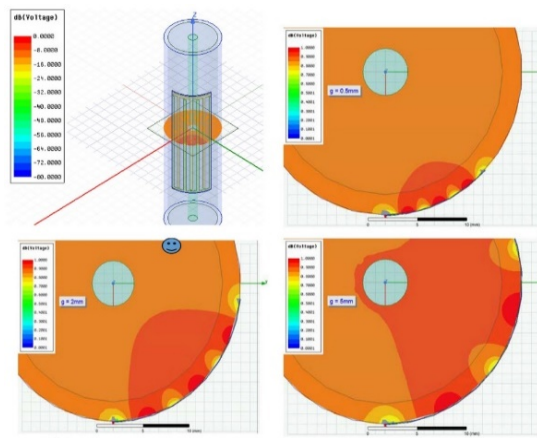


Figure 2-23. Finite element simulation of field penetration depth (red) as a function of time (yellow) gap (upper right – tight; lower left-medium, lower right-wide tine gap. (Glass III et al. 2018)



Figure 2-24. Pink EPR insulation; CPE jacket aged samples with jacket removed from half of the sample (Glass III et al. 2018)

each sample the jacket was stripped off to allow a direct IDC measurement on the insulation. On the other half, the jacket was left on so that the IDC measurement could be made, and the condition of the insulation inferred based on the dual sensor measurements with the sensor only in contact with the jacket. The predicted vs. measured values agreed quite well as indicated by an  $R^2$  value of 0.98 (where perfect correlation would be 1.00) (Figure 2-25). This is the only known test that can assess the insulation condition through a polymer jacket and adds to the appeal of an IDC measurement approach.

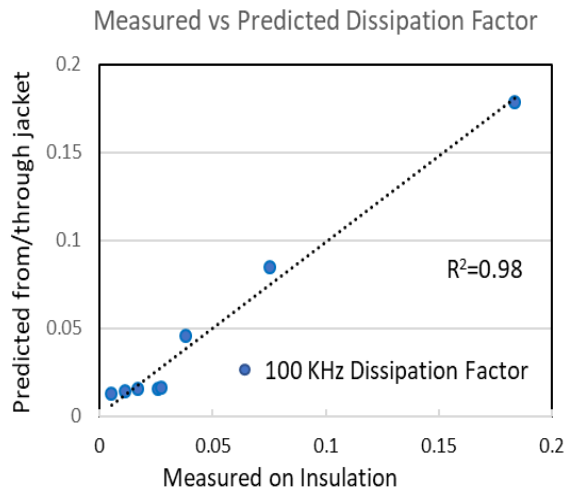


Figure 2-25. Linear least squares correlation of measured (on-insulation) vs. predicted (through jacket) dissipation factor which is shown to indicate insulation condition

### 3. Examples of Online monitoring Fault Detection

#### 3.1 TDR Rod Control System Coil and Cable Testing in an NPP

An NPP experienced a blown fuse in a control rod drive mechanism power supply circuit, which allowed a control rod to drop into the reactor core causing an unplanned reactor shutdown (Caylor et al. 2019). No rod control cable anomalies were measurable when testing at cold shutdown conditions during the forced outage. Time domain reflectometry (TDR) measurements acquired while the plant was operating at 100% power located a short circuit between a control rod gripper coil cable and the steel of the reactor assembly (Figure 3-1). This short circuit was only detectable due to temperature and vibration caused by reactor operation. Distance to fault information was acquired using TDR data and the failed cable segment that had an exposed conductor from insulation damage was replaced.

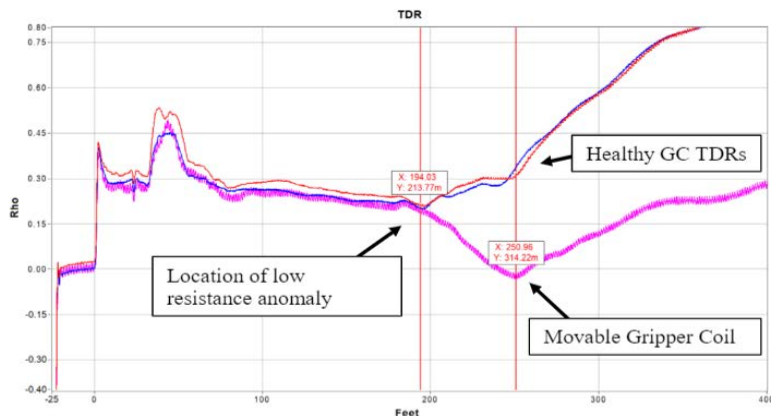


Figure 3-1. TDR traces locating a movable gripper coil short circuit on reactor head

#### 3.2 TDR Intermittent Fault Identification in a Nuclear Power Plant Instrument Cable

In another NPP application, a cable testing system is described that could be connected to an active, low frequency circuit and continuously monitor electrical characteristics using the time domain reflectometry (TDR) technique until an intermittent impedance change occurs (McConkey, Ryan, and Harmon 2017). This technique uses the difference in frequency response of the circuit and the TDR to isolate the TDR signature from the active circuit data. When a momentary impedance change occurs that exceeds a preconfigured limit threshold, the distance to fault data is automatically overlaid with the healthy baseline reference and stored in a database for diagnosis and repair.

Fluctuations in the reactor containment temperature were adversely affecting the signal output of source range neutron detectors. Plant data indicated that spiking occurred in the wide range and source range nuclear instrumentation system (NIS) channels when the temperature of the reactor building exceeded a certain threshold. When the containment temperature dropped below this value, the spiking stopped. The spiking returned when the reactor building temperature increased again. Because of the intermittent nature of the problem, troubleshooting involved repeated testing of the NIS circuit. Eventually, it was determined that the problem was in the reactor containment penetration which was subsequently replaced. A system that could continuously monitor the electrical properties of a cable circuit and identify the location of changes could have significantly reduced outage time and greatly reduced the time needed to return the nuclear instrumentation circuit to normal operation. A laboratory circuit was setup to simulate the field condition and demonstrate the system's ability to detect and locate the type of flaws that were assumed to be causing the plant's intermittent fault indications (Figure 3-2).

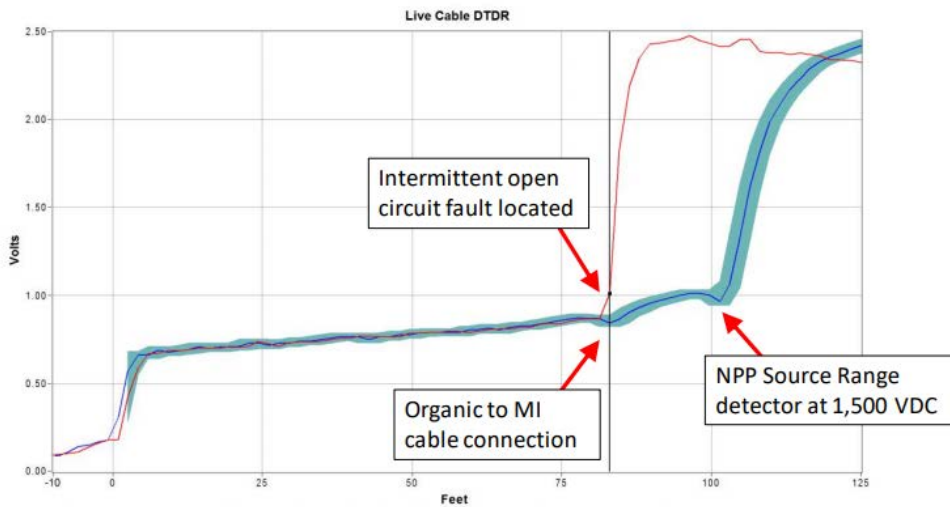


Figure 3-2. Intermittent fault location in an energized source range neutron detector circuit at 1,500 VDC normal operating voltage in laboratory test environment

### 3.3 MV Partial Discharge Monitoring/Trending with Cable as Waveguide

(Cuppen A.N. 2010) presented PD trends of various developing faults such as drying out of impregnated paper cables, moisture ingress, earth screen damage, etc. These trends were measured over either weeks, or months, by online PD measurement instrumentation with capability to also locate the source of PD activity. The presented cases included results from continuous measurements on more than 150 cable connections. The specific PD online monitoring with location instrumentation consists of a sensor/injector unit and control unit set coupled to the cable at each end. The sensor/injector unit contains both a sensor to measure pulses from the cable, and an injector, to inject pulses into the cable. The injected pulses are used for synchronization, local impedance measurements and online TDR. The sensor/injector unit is clamped around the cable termination or cable earth connection. This can be done while the cable remains in service. An optical fiber link connects the two units. The control unit is a small dedicated computer which controls the measurement sequence, the data collection, the signal processing, and the communication. On-board communication (LAN, modem, or mobile phone) facilities upload of the resulting data via the internet to a control center for further interpretation and for remote access and updates. No physical access to the units is needed once installed.

In one example a fault within a crimp connector joint at 1,678 m in a 4,258 m long MV cross-linked polyethylene (XLPE) insulated cable circuit was detected. Figure 3-3 shows the 3-D graph of 20 days of measurements on this circuit. Over a period of 3 weeks the PDs disappeared and reappeared. The PD origin was very narrow. The network owner was advised of the PD detection and recommended to replace the joint. For operational considerations, the joint was left in service until failure ~ 20 days after initial PD detection.

Observations and conclusions from this paper include:

- The discharge frequency (number of discharges per second) and density vary significantly based on the type of developing fault. Some weak spots develop slowly, with a high frequency and intensity of PDs, while other weak spots develop suddenly.
- Online PD measurements were detectable, possible to locate well before a catastrophic failure, and the hourly or more frequent updates offer significant advantages over offline PD testing.

- Remote reporting to a central location manned by experts helped identify significant PD as opposed to noise or false alarm signals. The installed network allowed review of more than 100 cables in one morning.

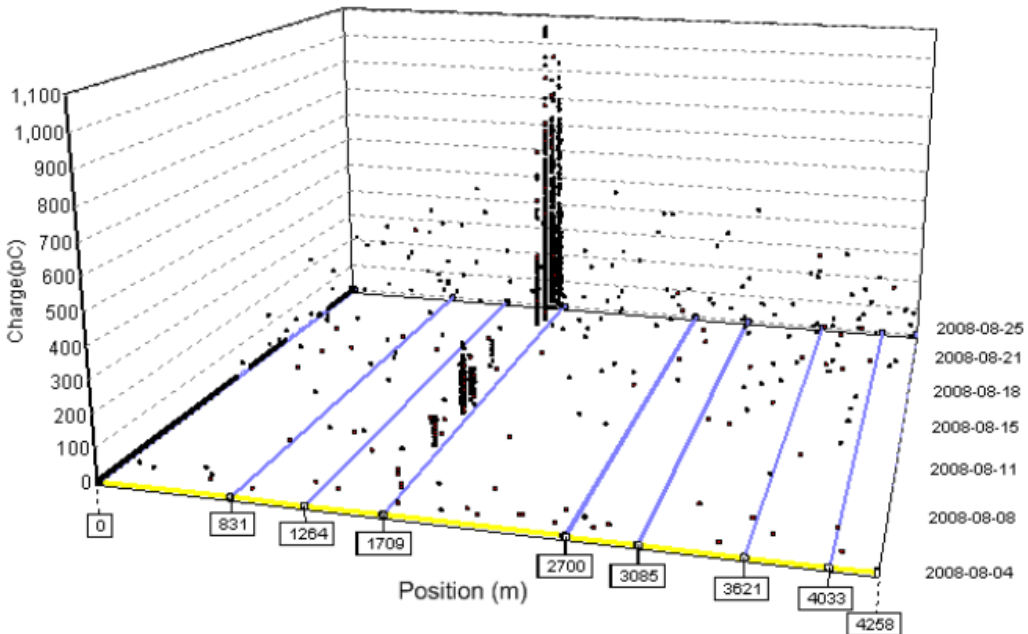


Figure 3-3. 3-D graph of developing PDs in a flawed joint with a crimped connector running hot at 1,678 m along the circuit length (Cuppen, Steennis, and van der Wielen 2010)

### 3.4 HV Fiber Optic Monitoring of Temperature Profile

In early 1998, a series of power failures occurred in the underground cables providing electricity to the central business district of Auckland (Peck, Seebacher, and Optech 2000). Consequently, much of the city lost power for an extended period which had a significant impact on economic activity. Post-failure analysis concluded that ‘this disastrous power failure …(with) consequential costs exceeding hundreds of millions of dollars might have been avoided had a distributed temperature sensor (DTS) been used to monitor for hot spots along the length of the cable’. They concluded that “Mercury Energy’s 110 kV cables had been operating at temperatures above their design limits from an early stage after their commissioning. In fact, the rating of these cables was much lower due to the ground conditions in which they were buried. When they were loaded to more than half their nominal rating, they would have started to overheat.”

When the replacement cables were installed in December of 1998 the vendor incorporated a fiber optic DTS and, as part of their contract, provided a monthly report on circuit performance to the utility using data from the DTS sampled every 2 hours and load information from the power company. This continuous monitoring, with data resolution of 2 m along the cable, has shown that there are certain regions along the 9 km route that are warmer than the average and these segments bear additional operational scrutiny.

DTSs are sufficiently common and accepted such that the IEEE has developed a standard (IEEE 2012) providing guidance on cable temperature measurements in general and particularly focusing on distributed fiber optic temperature measurement. The standard stipulates “the performance claims of the DTS manufacturer (accuracy, spatial resolution, measurement time, temperature resolution, etc.) are confirmed by tests made by the DTS manufacturer, based on a stated fiber specification and published in the technical specification giving the performance of the DTS.” Specific performance parameters are

suggested including temperature range, accuracy, spatial resolution, distributed measurement length, and update frequency. One of the main reasons for a DTS is to allow operators to maximize the system ampacity while protecting the cable from damage or failure. The ampacity limits of these systems are based on the maximum allowable temperature of the insulation. Typical ampacity limits are based on generalized and assumed worst expected conditions. A temperature monitoring system, appropriately applied, provides real-time temperature information to the user that may permit adjusting the current limits for both continuous and emergency conditions while assuring that conductor temperatures do not exceed allowable limits.

### 3.5 Fiber Optic Monitoring of PD

A fiber optic system described by (Tian et al. 2005) was installed on a 132 kV line and on a 400 kV line in a controlled laboratory test facility where more than one fault was detected and forensically analyzed. The specific fiber optic system configuration included an optically based remote sensing technique using a laser source, polarization scrambler, standard single mode fibers, fiber polarizer, electro-optic modulator and an optical receiver. It was designed for continuous online monitoring of PDs along the cable and particularly in the cable joints. The main

insulation material of the 132 kV cable joint was EPR whereas the cable insulation was XLPE. The cable ends were connected to oil-filled terminations. Conducting paint in the shape of a 'v' was deliberately applied on top of the cable XLPE between the cable joint stress cone conductor and the cable joint outer semiconducting layer to act as a PD source within the cable joint. As the voltage was stepped up while monitoring for PD, concurrent PD measurements from both a conventional electrical PD detector and the fiber optic detector were monitored. The PD level was  $\sim 100\text{--}130 \text{ pC}$  at 40 kV, and  $\sim 250\text{--}280 \text{ pC}$  at 60 kV. The two signal responses (at 40kV and 60kV) were similar in shape but with proportionally increased level at 60 kV (Figure 3-4).

For the 400 kV line, a prefabricated 220 kV to 400 kV composite joint type was applied. It consisted of an insulating body made of epoxy resin with an integrated field control electrode. A conventional PD electrical sensor as well as the fiber optic PD sensor was installed for these laboratory tests. As test voltages were increased to 41 kV, PD was detected using the fiber optic PD detection system (Figure 3-5). After-test inspection indicated that the PD activity was due to a manufacturing production defect void between the cable conductor and the epoxy resin within the cable joint.

The 400 kV cable joint was replaced and the loop was re-energized. It was PD free for an applied voltage of 250 kV. Four metal wires were then placed on the surface of the stress cone near to the cable conductor, and the joint reassembled. PD measurements were then carried out using the fiber optic detector. High voltage was applied to the loop and in this case the PD inception voltage was found to be 13 kV. The voltage was further increased, and the resulting PD signal observed at 70 kV is shown in Figure 3-6.

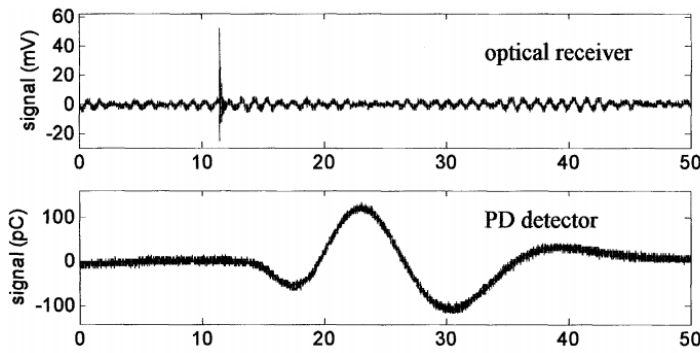


Figure 3-4. Fiber optic receiver signal and conventional partial discharge sensor responses to a 40 kV applied test voltage (Tian et al. 2005)

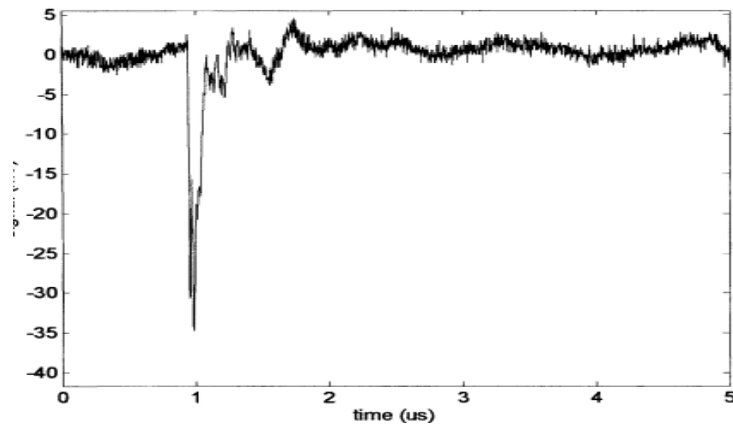


Figure 3-5. Optical sensor PD signal from real production defect (void) between stress shield and epoxy resin within the 400 kV cable joint  
(Tian et al. 2005)

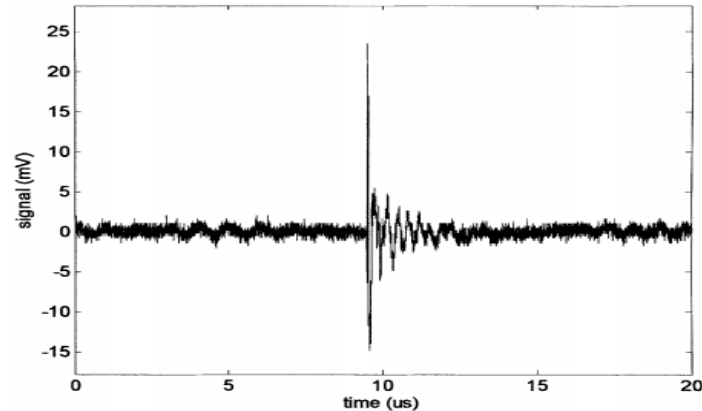


Figure 3-6. Optical sensor PD signal due to PD from wires within the cable joint of 400 kV cable at 70 kV (Tian et al. 2005)

## **4. Conclusions**

The feasibility for online monitoring to detect several cable fault types of interest has been established by a number of labs, universities, and commercial entities using a variety of methods. Among the techniques examined above, some are being applied to HV and critical-cable systems. Online techniques were also cited for diagnostics of intermittent cable related faults. Utilization of such methods may not only reduce condition monitoring and cable aging management costs but could increase operational safety and maintenance efficiency through enabling a larger fraction of plant cables to be assessed simultaneously. Additionally, developing the capability to test in-service cables while the plant is operating will save valuable time while the plant is shut down for maintenance outages. Broad application of these techniques however has not extended to MV and LV cable systems of industrial or nuclear plants as a common practice. Exploitation of these technologies for a broader range of cables will require additional research to reduce equipment, installation, and operating costs.

## 5. References

- Allil, Regina C. S. B., M.M. Werneck, Bessie A. Ribeiro, and F. V. B. de Nazaré. 2013. "Application of Fiber Bragg Grating Sensors in Power Industry." In *Current Trends in Short- and Long-period Fiber Gratings*, edited by Christian Cuadrado-Laborde. Argentina: National Scientific and Technical Research Council.
- AP Sensing. 2020a. "Distributed Temperature Sensing, newly defined: Designed for the most demanding applications." AP Sensing, accessed 5/10/20.  
[https://www.apsensing.com/fileadmin/landingpages/dtsn45series/downloads/Flyer\\_DTS\\_N45-Series.pdf](https://www.apsensing.com/fileadmin/landingpages/dtsn45series/downloads/Flyer_DTS_N45-Series.pdf)
- AP Sensing. 2020b. "DTS (Distributed Temperature Sensing)." <https://www.apsensing.com/technology/dts>
- Arvia, E. M., R. T. Sheldon, and N. Bowler. 2014. "A capacitive test method for cable insulation degradation assessment." 2014 IEEE Conference on Electrical Insulation and Dielectric Phenomena (CEIDP), 19-22 Oct. 2014.
- Bowler, N, and Shuaishuai Liu. 2015. "Aging Mechanisms and Monitoring of Cable Polymers." *International Journal of Prognostics and Health Management* 6:1-12.
- Campanella, C. E., A. Cuccovillo, C. Campanella, A. Yurt, and V. M. N. Passaro. 2018. "Fibre Bragg Grating Based Strain Sensors: Review of Technology and Applications." *Sensors (Basel)* 18 (9). doi: 10.3390/s18093115.
- Caylor, S.D., J.B. McConkey, G.W. Morton, and H.M. Hashemian. 2019. "On-line Monitoring and Diagnostics for Rod Control Systems in Nuclear Power Plants."
- Chakraborty, S. 2017. *Condition Monitoring of Power Cables using Partial Discharge*. Edited by Lambert Academic Publishing. Republic of Moldova: lambert Academic Publishing.
- Chen T., Bowler N., Bowler J. 2012. "Analysis of Arc-Electrode Capacitive Sensors for Characterization of Dielectric Cylindrical Rods." *IEEE T. Instrumentation and Measurement* 61:233-240. doi: 10.1109/TIM.2011.2157573.
- Chung Y., Amarnath N., Furse C. 2009. "Capacitance and Inductance Sensor Circuits for Detecting the Lengths of Open- and Short-Circuited Wires" *IEEE TRANSACTIONS ON INSTRUMENTATION AND MEASUREMENT* 58 (8).
- Chung, Y. C., N. N. Amarnath, and C. M. Furse. 2009. "Capacitance and Inductance Sensor Circuits for Detecting the Lengths of Open- and Short-Circuited Wires." *IEEE Transactions on Instrumentation and Measurement* 58 (8):2495-2502. doi: 10.1109/Tim.2009.2014617.
- Cuppen A.N., Steennis E.F., Van der Wielen P.C. 2010. "Partial Discharge Trends in Medium Voltage Cables measured while in-service with PDOL." IEEE Transmission and Distribution Conference and Exhibition.
- Cuppen, Andrew N., E. Fred Steennis, and Peter C. J. M. van der Wielen. 2010. "Partial Discharge Trends in Medium Voltage Cables measured while in-service with PDOL." IEEE Transmission and Distribution Conference and Exhibition.

- Dakin, J. P., D. J. Pratt, G. W. Bibby, and J. N. Ross. 1985. "Distributed Antistokes Ratio Thermometry." Optical Fiber Sensors, San Diego, California, 1985/01/01.
- Duckworth, Gregory, and Emery Ku. 2013. "OptaSense (R) distributed acoustic and seismic sensing using COTS fiber optic cables for Infrastructure Protection and Counter Terrorism." *Proc SPIE*. doi: 10.1117/12.2017712.
- Farahani, M. A., and T. Gogolla. 1999. "Spontaneous Raman scattering in optical fibers with modulated probe light for distributed temperature Raman remote sensing." *Journal of Lightwave Technology* 17 (8):1379-1391. doi: 10.1109/50.779159.
- Fifield, L S, M P Westman, A Zwoster, and B Schwenzer. 2015. Assessment of Cable Aging Equipment, Status of Acquired Materials, and Experimental Matrix at the Pacific Northwest National Laboratory. Richland, Washington: Pacific Northwest National Laboratory.
- Froggatt, M., and J. Moore. 1998. "High-spatial-resolution distributed strain measurement in optical fiber with rayleigh scatter." *Appl Opt* 37 (10):1735-40. doi: 10.1364/ao.37.001735.
- Furse, C., Y. Chung, C. Lo, and P. Pendayala. 2006. "A critical comparison of reflectometry methods for location of wiring faults." *Smart Structures and Systems* 2 (1):25-46.
- Furse C., Chung Y., Lo C., Pendayala P. 2006. "A critical comparison of reflectometry methods for location of wiring faults." *Smart Structures and Systems* 2 (1):25-46.
- Furse, C., Y. Chung, D. Rakesh, M. Nelsen, G. Mabey, and R. Woodward. 2003. " Frequency Domain Reflectometry for On Board Testing of Aging Aircraft Wiring." *IEEE Trans. Electromagnetic Compatibility* 45 (2):306-315.
- Furse, C., P. Smith, M. Safavi, and C. Lo. 2005. "Feasibility of spread spectrum sensors for location of arcs on live wires." *EEE Sensors* 5 (6): 1445-1450.
- Galindez-Jamioy, C. A., and J. M. López-Higuer. 2012. "Brillouin Distributed Fiber Sensors: An Overview and Applications." *Journal of Sensors*.
- Glass III, S W, L S Fifield, N Bowler, A Sriraman, and W C Palmer. 2018. Interdigital Capacitance Local Non-Destructive Examination of Nuclear Power Plant Cable for Aging Management Programs. Richland, Washington: Pacific Northwest National Laboratory.
- Glass, S W, L S Fifield, G Dib, J R Tedeschi, A M Jones, and T S Hartman. 2015. State of the Art Assessment of NDE Techniques for Aging Cable Management in Nuclear Power Plants FY2015. Richland, Washington: Pacific Northwest National Laboratory.
- Glass, S W, L S Fifield, and T S Hartman. 2016. Evaluation of Localized Cable Test Methods for Nuclear Power Plant Cable Aging Management Programs. Richland, Washington: Pacific Northwest National Laboratory.
- Glass, S W, A M Jones, L S Fifield, and T S Hartman. 2016. Distributed Electrical Cable Non-Destructive Examination Methods for Nuclear Power Plant Cable Aging Management Programs. Richland, WA: Pacific Northwest National Laboratory.
- Glass, S W, A M Jones, L S Fifield, T S Hartman, and N Bowler. 2017. Physics-Based Modeling of Cable Insulation Conditions for Frequency Domain Reflectometry (FDR). Richland, Washington: Pacific Northwest National Laboratory.

- Glass, S. W., M. N. Al-Imran, L. S. Fifield, and M. Ali. 2019. "Simulation and Experimental Results of Interdigital Capacitor (IDC) Sensors to Monitor Insulation Degradation of Cables." 2019 IEEE Conference on Electrical Insulation and Dielectric Phenomena (CEIDP), 20-23 Oct. 2019.
- Glass, S.W., L.S. Fifield, N. Bowler, A. Sriraman, and C. Gifford. 2019. PNNL 29092 Dielectric Spectroscopy for Bulk Condition Assessment of Cable Insulation. Pacific Northwest National Laboratories.
- Hashemian, H. M. 2012. "Testing old cables." *Nuclear Engineering International* 57 (697):32-33.
- HV Diagnostic Technologies. 2019. "The Basics of Partial Discharge Testing." <https://hvtechnologies.com/blog/basics-partial-discharge-testing>.
- IAEA. 2012. Assessing and Managing Cable Ageing in Nuclear Power Plants. Vienna: International Atomic Energy Agency (IAEA).
- IEEE. 2012. IEEE Std. 1718 Guide for Temperature Monitoring of Cable Systems. New York NY: IEEE.
- Igreja, R, and C.J Dias. 2004. "Analytical evaluation of the interdigital electrodes capacitance for a multi-layered structure." *Sensors and Actuators A: Physical* 112 (2-3):291-301.
- Imran, Md Nazmul Al, Samuel W. Glass, Leonard S. Fifield, and Mohammod Ali. 2020. "Flexible Fabric Based IDC Sensors for Conformal Curved Surface Applications." *IEEE Sensors Journal*:1-1. doi: 10.1109/jsen.2020.3015156.
- Konig, D., and Y.N. Rao. 1993. *Partial Discharges in Electrical Power Apparatus*. Berlin: VDE Verlag.
- Lumens, P., A. Franzen, K. Hornman, S. Grandi, G. Hemink, B. Kuvshinov, J. La Follett, B. Wyker, and P. Zwartjes. 2013. "Cable development for Distributed Geophysical Sensing, with a field trial in surface seismic." *Proc SPIE*. doi: 10.1117/12.2025693.
- Lumens, P. G. E. 2014. Fibre-optic sensing for application in oil and gas wells. Technische Universiteit.
- Mamishev, R.V., K. Sundara-Rajan, F. Yang, Y. Du, and M. Zahn. 2004. "Interdigital sensors and transducers." *Proceedings of the IEEE* 92 (5).
- Marmon. 2019. "Power Cable Monitoring." Marmon/Berkshire Hathaway Co. <https://www.marmonsensing.com/Applications/Power-Cable-Monitoring>.
- McConkey, J.B., K.M. Ryan, and G.R. Harmon. 2017. "Identification and Repair of Intermittent Cable Faults in Nuclear Power Plants." NPIC&HMIT, San Francisco, CA.
- Megger. 2020. "TDR900 Hand-held Time Domain Reflectometer/Cable Length Meter." <https://www.globaltestsupply.com/pdfs/cache/www.globaltestsupply.com/tdr900/datasheet/tdr900-datasheet.pdf>
- MIL 1553. 1976. MIL Std 1553 Aircraft Internal Time Division Command/Response Multiplex Data Bus.
- Mohr and Associates. 2009. Mohr Operator's Manual for CT100 and CT100HF. Richland, Washington: Mohr and Associates.
- Mohr and Associates. 2010. Application Note: TDR vs. FDR: Distance-to-Fault. Richland, Washington: Mohr and Associates.

- Naik, S, C.M. Furse, and B.F. Boroujeny. 2006. "Multicarrier Reflectometry." *IEEE Sensors Journal* 6 (3): 812-818.
- Nikitin, S. P., A. I. Kuzmenkov, V. V. Gorbuleko, O. E. Nanii, and V. N. Treshchikov. 2018. "Distributed temperature sensor based on a phase-sensitive optical time-domain Rayleigh reflectometer." *Laser Physics* 28 (8). doi: 10.1088/1555-6611/aac714.
- Nikles, M., Bosson, R. 2009. "Long-distance fiber optic sensing solutions for pipeline leakage, intrusion and ground movement detection." *Proceedings of SPIE - The International Society for Optical Engineering* 7316. doi: 10.1117/12.818021.
- Nikles, M., B. Vogel, F. Briffod, S. Grosswig, F. Sauser, S. Luebbecke, A. Bals, and T. Pfeiffer. 2004. "Leakage detection using fiber optics distributed temperature monitoring." *Proc SPIE* 5384. doi: 10.1117/12.5400270.
- Optasense. 2016. "ODH-4 DAS Interrogator Unit." accessed 05/10/20. [https://www.optasense.com/wp-content/uploads/2017/05/TO\\_ODH-4\\_InterrogatorUnit\\_Overview\\_Digital\\_LR.pdf](https://www.optasense.com/wp-content/uploads/2017/05/TO_ODH-4_InterrogatorUnit_Overview_Digital_LR.pdf)
- Optics, OZ. 2016. "Distributed Strain and Temperature Sensing in Public Utilities." OZ Optics. [https://www.ozoptics.com/ALLNEW\\_PDF/PPT0021.pdf](https://www.ozoptics.com/ALLNEW_PDF/PPT0021.pdf)
- Peck, D., P. Seebacher, and T. Optech. 2000. "Distributed Temperature Sensing using Fibre-Optics (DTS Systems)." Electrical Engineers Anual Conference Aukland New Zealand, Aukland New Zeland.
- Rajeev, Pat, Jayantha Kodikara, W.K. Chiu, and Thomas Kuen. 2013. " Distributed Optical Fibre Sensors and Their Applications in Pipeline Monitoring." *Key Engineering Materials*. doi: 0.4028/www.scientific.net/KEM.558.424.
- Ramuhalli, P, L S Fifield, M S Prowant, G Dib, J R Tedeschi, J D Suter, A M Jones, M S Good, S W Glass, and A F Pardini. 2015. Assessment of Additional Key Indicators of Aging Cables in Nuclear Power Plants -- Interim Status for FY2015. Richland, Washington: Pacific Northwest National Laboratory.
- Rashdan, A., A. J. Smith, S. St. Germain, C. Ritter, V. Agarwal, R. Boring, T. Ulrich, and J. Hansen. 2018. INL/EXT-18-52206 ,Development of a Technology Roadmap for Online Monitoring of Nuclear Power Plants. Idaho National Laboratory.
- Rogers, A. J., and V. A. Handerek. 1992. "Frequency-derived distributed optical-fiber sensing: Rayleigh backscatter analysis." *Appl Opt* 31 (21):4091-5. doi: 10.1364/AO.31.004091.
- Sheldon, R. T., and N. Bowler. 2014. "An Interdigital Capacitive Sensor for Nondestructive Evaluation of Wire Insulation." *IEEE Sensors Journal* 14 (4):961-970. doi: 10.1109/Jsen.2014.2301293.
- Simmons, K L, L S Fifield, M P Westman, J R Tedeschi, A M Jones, M S Prowant, A F Pardini, and P Ramuhalli. 2014. Determining Remaining Useful Life of Aging Cables in Nuclear Power Plants – Interim Study for FY2014. Richland, Washington: Pacific Northwest National Laboratory.
- Simmons, K L, P Ramuhalli, D L Brenchley, and J B Coble. 2012. Light Water Reactor Sustainability (LWRS) Program – Non-Destructive Evaluation (NDE) R&D Roadmap for Determining Remaining Useful Life of Aging Cables in Nuclear Power Plants. Richland, Washington: Pacific Northwest National Laboratory.

- Smith, P. . 2003. Spread Spectrum Time Domain Reflectometry (Ph.D. dissertation). Utah State University.
- Smith, P., C. Furse, and P. Kuhn. 2008. "Intermittent Fault Location on Live Electrical Wiring Systems." *SAE International*.
- Tian, Y., P. L. Lewin, J. S. Wilkinson, G. Schroeder, S. J. Sutton, and S. G. Swingler. 2005. "An improved optically based PD detection system for continuous on-line monitoring of HV cables." *Ieee Transactions on Dielectrics and Electrical Insulation* 12 (6):1222-1234. doi: Doi 10.1109/Tdei.2005.1561802.
- Tsai, P., Y. Chung, C. Lo, and C. Furse. 2005. "PMixed Signal Reflectometer Hardware Implementation for Wire Fault Location." *IEEE Sensors Journal* 5 (6):1479-1482.
- Zaretsky, M. C., L. Mouayad, and J. R. Melcher. 1988. "Continuum Properties from Interdigital Electrode Dielectrometry." *IEEE Transactions on Electrical Insulation* 23 (6):897-917. doi: Doi 10.1109/14.16515.